UNIVERSITY OF CALIFORNIA,
IRVINE

Immunomodulation in wound healing

DISSERTATION

submitted in partial satisfaction of the requirements
for the degree of

DOCTOR OF PHILOSOPHY

in Biomedical Engineering

by

Raji Rao Nagalla

Dissertation Committee:
Associate Professor Wendy F. Liu, Chair
Professor Elliot Botvinick
Assistant Professor S. Armando Villalta

2020

DEDICATION

"The wound is where the light enters you" -Rumi

I dedicate my dissertation to the many teachers and mentors who encouraged my curiosity and guided my passion for learning towards the medical sciences.

To my parents, my first teachers, who provided me countless opportunities to explore the world around me, from getting my hands dirty on the farm in Oregon to the affording me the privilege of a robust education. I am grateful for your sacrifices and your steadfast support, every day.

Next, to my grade school mentors, who enticed me first with kitchen science experiments and then with yearlong science fair projects from 6th through 12 grade, each culminating in a full scientific report and exhibition at the science fair. These formative years instilled the value of the scientific method in my bones, and taught me the fundamentals of communicating my findings with the public and scientific communities.

To my peers, faculty, and staff at Wellesley College, who shaped my academic and personal growth in an environment unencumbered by the confines of patriarchal gender roles. I especially acknowledge my honors thesis advisor, Dr. Nancy H. Kolodny, who supported my first formal exploration of interdisciplinary science, paving the way for this dissertation and my pursuit of a career at the intersection of science and medicine.

Finally, to my mentorship team at UCI, all of whom have supported me through the transitions and tumult of my time in the MSTP, enabling my success in the first two years of medical school, and now in graduate school. As a boundary pusher, I am thankful for the wealth of advice provided by senior students, research advisors and my clinical mentors. Together, I believe we can do anything.

TABLE OF CONTENTS

Page

LIST OF FIGURES

ACKNOWLEDGEMENTS

I thank my advisor, Dr. Wendy F. Liu, for her guidance and the opportunity to pursue these projects during my PhD training, and my thesis committee members, Dr. Elliot Botvinick and Dr. S. Armando Villalta, for their guidance as I developed and executed my project. Thank you also to Dr. Maksim Plikus, whose expertise in skin wound healing has proven invaluable. I appreciate the countless hours spent by my many peers and colleagues at UCI and beyond, who shared reagents, protocols, and feedback, and listened to my developing story at every step along the way.

I am grateful to my MSTP family, the faculty, staff, and peers who share this road, for providing me logistical, emotional, and academic support whenever I reach out. It is truly my privilege to take part in this community. To my Wellesley community, thank you for being by my side every day, supporting me from across oceans and time zones. Most importantly, I thank my family, for their tireless support and belief in my abilities. I am here today because of you.

VITA

Raji Rao Nagalla

2014	B.A. in Biological Chemistry, Wellesley College
2014-present	MSTP (MD/PhD) student, University of California, Irvine SOM
2019	M.S. in Biomedical Engineering University of California, Irvine
2020	Ph.D. in Information and Computer Science, University of California, Irvine

FIELDS OF STUDY

Biomaterial Engineering

Innate Immunology

Wound Healing

PUBLICATIONS

Nagalla, R., Liao, Z.W., Webb, A., Flynn, N., and Kolodny, N. (2014). Functionalizing silica-coated iron oxide nanoparticles for imaging and targeted cancer therapeutics (780.3). FASEB J 28, 780.783.

Smith, T.D., Nagalla, R.R., Chen, E.Y., and Liu, W.F. (2017). Harnessing macrophage plasticity for tissue regeneration. Adv Drug Deliv Rev.

Rowley, A.T., Nagalla, R.R., Wang, S.W., and Liu, W.F. (2019). Extracellular Matrix-Based Strategies for Immunomodulatory Biomaterials Engineering. Adv Healthc Mater, e1801578.

ABSTRACT OF THE DISSERTATION

Immunomodulation in wound healing

by

Raji Rao Nagalla

Doctor of Philosophy in Biomedical Engineering

University of California, Irvine, 2020

Associate Professor Wendy F. Liu, Chair

There is a large and growing clinical need for improved wound therapies. Skin wound healing involves the orchestrated communication and activities of macrophages with other wound effectors. Wound macrophages and fibroblasts respond dynamically to changes in their local physical and biochemical environment, presenting a target for engineered biomaterials to modulate cell-cell interaction in the wound bed. This dissertation examines the reciprocal signaling between macrophages and fibroblasts, and the potential of biophysical properties of engineered hydrogels to modulate this interaction to improve wound healing. Soft gelatin methacrylate (gelMA) hydrogel was shown to reduce scar size in small, full-thickness murine skin wounds, compared to stiff gelMA and no-treatment, additionally promoting a pro-healing macrophage phenotype *in vitro* and *in vivo*. Single-cell RNA sequencing of wound tissue treated with soft or stiff gelMA or no material at post wound day 5 revealed heterogeneous macrophage and fibroblast populations, with distinct shifts and differential gene expression in response to material stiffness. Cell-based wound closure assays in 2D and 3D were used to further parse these interactions, showing that juxtacrine co-culture of murine bone marrow derived macrophages with NIH 3T3 fibroblasts significantly enhanced fibroblast closure of 2D and 3D wounds. Coculture also altered macrophage activation in a contact-dependent manner, when compared to culture of ether cell type alone. Finally, broad inhibition of gap junctions with

palmitoleic acid abrogated fibroblast enhanced macrophage IL-10 secretion and coculture enhanced calcium activity, suggesting that cell-cell contact through gap junctions may, in part, mediate macrophage-fibroblast communication. This work demonstrates a critical role for direct macrophage-fibroblast interactions in the cellular coordination of wound healing, and reveals the potential for targeting biophysical immunomodulation in the development of wound healing therapeutics.

INTRODUCTION

In health and disease, macrophages regulate immune homeostasis in almost every tissue of the body. These innate immune cells respond to diverse physical stimuli in their microenvironment, and direct immune and stromal cell response following injury or implantation of biomaterials. The increasing prevalence of metabolic and cardiovascular disease, as well as surgical interventions, contribute to a growing clinical need to repair tissues, which has yet to be addressed therapeutically. Many mechanistic determinants of healing remain unknown, hindering the development of material treatments, particularly those that ally with the host immune system. Current biomaterial treatments largely serve to occlude the injured tissue, although some target angiogenesis and formation of granulation tissue. Synthetic and tissue-derived materials additionally encounter some level of unwanted inflammation due to foreign body response (FBR). Wound dressings and biomaterial implants provide biophysical cues that could potentially direct macrophage regulation of both FBR and tissue repair. The critical role of macrophages in both wound healing and FBR makes them an ideal target for therapeutic exploration. This introduction describes recent work and observations made in translational studies exploring the material-mediated modulation of macrophages in wound healing. We begin with an overview of the *in vitro* studies, and then review the animal and clinical studies that, together, hold the potential to uncover therapeutic targets for molecular and materials engineering.

Role of macrophages in tissue repair and the foreign body response

Macrophages orchestrate the wound healing response by coordinating transitions in biochemical cues between stages (Kloc et al., 2018). Immediately following injury, macrophages follow neutrophils from the bloodstream to the wounded tissue, where local signals, including fragments of damaged cells and bacterial lipopolysaccharide (LPS), provoke inflammatory macrophage cytokine secretion. These factors include tumor necrosis factor alpha (TNFα),

interleukin 1 beta (IL-1β), interferon gamma (IFNγ), and chemokine CCL22. This milieu recruits other immune cells and stromal cells that play a role in the healing response. The transition from the inflammatory to the proliferative phase of wound healing is marked by the appearance of anti-inflammatory macrophages, secreting IL-10, transforming growth factor beta (TGFβ), vascular endothelial growth factor (VEGF), and other pro-healing factors. It is suspected that microenvironmental cues, including mechanical properties, regulate recruitment of and plastic macrophage transformation into these anti-inflammatory macrophages, which then coordinate the multicellular healing response (Wong et al., 2011). In the final phase of wound healing, macrophages promote matrix deposition and remodeling, achieving closure with either functional tissue or scar. In the skin, fibroblasts are the primary stromal cell responsible for matrix deposition, tissue regeneration, and mechanical contraction of the wound to achieve closure (Witherel et al., 2016). Macrophages control fibroblast phenotype through the secretion of many soluble factors, including TGFβ, a contractile myofibroblast promoting factor. Myofibroblast-mediated circumferential tension at the wound edge may in fact reduce mechanical tension on the wound bed, facilitating proliferation and resolution (Pensalfini et al., 2018; Sakar et al., 2016). Over the course of wound healing, the stiffness of the wound bed increases from the 3-5 kPa to ~50 kPa, as observed in rat skin wounds over 7 weeks (Goffin et al., 2006). Physical and biochemical cues differentiate healthy healing from pathologic fibrosis and scar formation, where stiffness can reach in excess of 150 kPa. Engineering of biomaterial treatments to take advantage of dynamic mechanosensing at the wound site is hindered, as the mechanisms governing the myofibroblast-macrophage-matrix interactions that decide the fate of a wound remain loosely defined (Pakshir and Hinz, 2018; Smith et al., 2017).

At the extremes, the body responds to injury with a regenerative or fibrotic process, and ongoing work aims to characterize the complex macrophage populations in these distinct biophysical environments (Sommerfeld et al., 2019). Increasingly, Omics tools, such as RNAseq,

are being used to understand the complex and heterogeneous tissue response to biomaterials. Studies *in vitro, in vivo,* and in human trials all contribute to informing biomaterial engineering of new wound therapies, and will be discussed in this chapter. FBR and wound healing both present an unmet clinical need for novel engineered materials. Targeting macrophage mechanobiology may lead to development of materials that can ultimately take advantage of the host immune system to foster regeneration.

Modulation of macrophage function via physical biomaterial properties *in vitro*

Biomaterial engineering begins at the bench, from synthesizing the material itself to initial testing of its effects in a biological context. Cell studies in 2D and 3D provide critical information on toxicity and contamination, in a high throughput fashion. Isolation of physical and biochemical parameters in vitro also allows for mechanistic insight that can be confounded in more complex animal and clinical systems. Macrophage mechanobiology is an emerging field, and uniquely benefits from the breadth of *in vitro* engineering approaches to understanding cell behavior. In this section, we describe what is currently known about macrophage modulation by physical material properties, and what remains to be explored (Fig. 1).

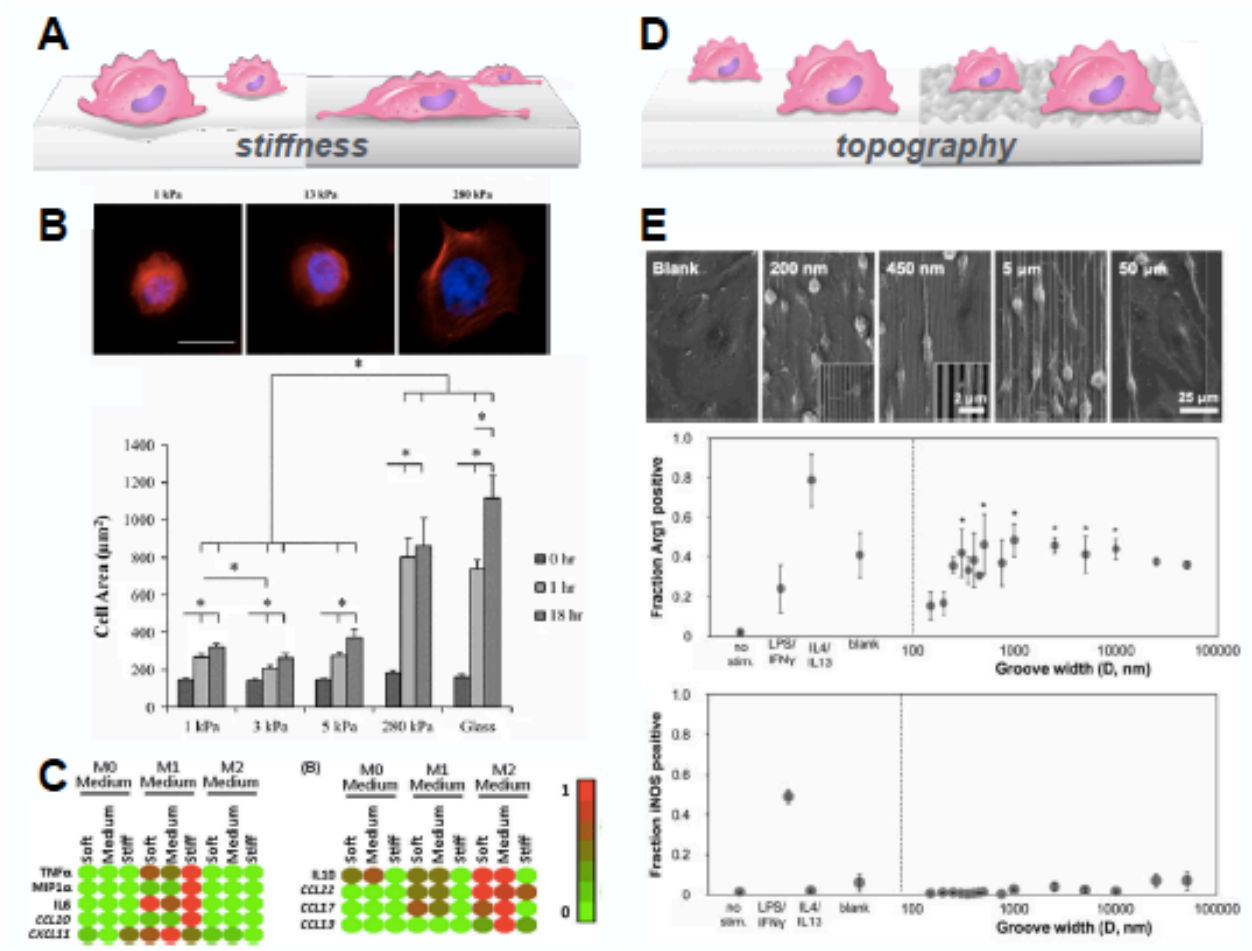

Figure 1. Effects of material stiffness and surface topography on macrophage behavior *in vitro*. (A) Schematic of macrophages on soft and stiff surfaces. (B) Human monocyte derived macrophages increase in cell area on substrates of increasing stiffness (Adlerz et al., 2016). (C) THP-1 macrophage cytokine secretion on collagen coated polyacrylamide substrates of varying stiffness, stimulated with none, IFNγ and LPS, or IL-4 and IL-13 cytokines (Sridharan et al., 2019a). (D) SEM images of BMDM cultured on titanium patterned with lines of varying width (top) and quantification of fraction of Arg1 or iNOS positive (bottom) (Luu et al., 2015). Figures adapted from Adlerz, 2016; Sridharan, 2019; Luu, 2015; Smith, 2017(Smith et al., 2017).

Biomaterial stiffness influences many macrophage behaviors, including motility, activation, cytokine production, proliferation, and lipid accumulation (Leifer et al., 2016; Sridharan et al., 2019a; Van Goethem et al., 2010). Macrophages from a variety of disease and tissue contexts have been cultured on a wide range of substrates, including non-degradable titanium and PCL (MPa-GPa), and collagen and alginate hydrogels (Pa - kPa) (Adlerz et al., 2016; Féréol et al., 2006; Hsieh et al., 2019). These materials vary widely, not only in their stiffness ranges, but

also their adhesive and biochemical properties, constraining interpretation of isolated stiffness effects when comparing studies. To more specifically examine the effects of stiffness, studies have used hydrogels with varied crosslinking density, which can be engineered with similar adhesive ligand presentation and physiologically relevant stiffness ranges. Current work has also begun to explore molecular mechanisms underlying mechanotransduction, which may ultimately lead to therapeutics aimed at controlling macrophage responses to different stiffness environments.

Many studies show that macrophage polarization tends towards an inflammatory phenotype on stiffer substrates(Hamlet and Ivanovski, 2017; Hsieh et al., 2019; Okamoto et al., 2018; Previtera and Sengupta, 2015; Sridharan et al., 2019a), although some groups have found a more variable response to stiffness depending on the material, stiffness range, phenotypic readout, and type of macrophage tested (Figure 1B) (Adlerz et al., 2016; Wouters et al., 2017). For example, both murine bone marrow derived macrophages (BMDM) (Previtera and Sengupta, 2015) and human THP-1 macrophages (Sridharan et al., 2019a) have been shown to secrete less TNFα on soft (0.3 - 11 kPa) protein coated polyacrylamide (PA) gels with LPS stimulation, compared to stiff (230 - 323 kPa) gels (Figure 1C). In contrast, Wouters and colleagues (Wouters et al., 2017) found no effect of substrate stiffness on polarization markers IL1β, CD40, CD206, or CD1b in human monocyte derived macrophages cultured on collagen-coated polyacrylamide hydrogels and stimulated with either LPS and IFNγ or IL-4 and IL-13 (Wouters et al., 2017). However, they did observe increased macrophage fusion into foreign body giant cells on 12 and 26 kPa gels compared to softer (4 kPa) and stiffer (92 kPa) gels (McWhorter et al., 2015; Wouters et al., 2017). Another study demonstrated decreased cytokine secretion by BMDM on soft (130 kPa) PEG-RGD hydrogels compared to stiff materials (840 kPa), suggesting that stiffness may not only alter macrophage polarization, but also control the extent of activation (Blakney et al., 2012). Complicating matters, the crosslinking agent used to modulate material stiffness may itself

skew macrophage response. Sridharan and colleagues (Sridharan et al., 2019b) showed that the collagen crosslinked with Genepin and dehydrothermal (DHT) processing suppressed activation of THP-1 macrophages compared collagen crosslinked with DHT alone, while 1-Ethyl-3-(3-Dimethylaminopropyl) carbodiimide (EDAC) and DHT crosslinking increased both inflammatory and anti-inflammatory activation. Perhaps because all of these gels ranged from 0.42 - 1.6 kPa, a small and soft stiffness range, there were no significant correlations between substrate stiffness and activation. Overall, there is compelling evidence that stiffer materials with similar biochemical composition increase macrophage inflammatory response, while the effect of soft substrates seems to depend on the material.

Cell-substrate signaling is complex and remains poorly understood in macrophages. Multiple groups have explored the possibility that stiffness mechanotransduction is mediated by mechanosensitive transmembrane structures. For example, culture of THP-1 macrophages encapsulated in 3 kPa IL-4 containing gelatin methacrylate (GelMA) hydrogels results in low inflammatory CD86 and high anti-inflammatory CD206 expression. Inhibition of integrin $\alpha 2\beta 1$ in this system, using blocking antibodies, moderately increases expression of CD86, and dramatically suppresses anti-inflammatory CD206 expression, suggesting that integrins may play a role in transducing mechanical signals in macrophages (Cha et al., 2017). In addition, the mechanosensitive ion channel TRPV4 potentiates LPS-induced IL-10 production and phagocytosis, inferred from reduced activity in BMDM and alveolar macrophages from TRPV4 knock out mice, but a specific role for this ion channel in stiffness sensing has not yet been identified (Scheraga et al., 2016). Expression and activity of LPS receptor TLR4 also increases with stiffness in BMDM grown on polyacrylamide hydrogels, and TLR4 deficient BMDM show suppressed IL-1β and IL-6 secretion at baseline and upon LPS stimulation (Gruber and Leifer, 2020; Previtera and Sengupta, 2015). Downstream, MyD88 expression and NF-κB transcription factor phosphorylation and nuclear translocation also increase with stiffness, suggesting one

possible mechanism for intracellular transduction of stiffness mediated inflammation. In contrast, inhibition of intracellular transduction factor PPARγ with antagonist GW9662 suppressed high anti-inflammatory CD206 expression in THP-1 macrophages on soft agarose gels, suggesting that this pathway may oppose the TLR4-mediated stiffness driven inflammation (Okamoto et al., 2018). Ongoing research into the diverse and heterogeneous macrophage response to substrates of varying stiffness may yield further mechanistic insights. Tissue stiffness and macrophage behavior play key roles in the pathophysiology of fibrosis and other disease processes, making mechanotransduction appealing fodder for molecular targeting of engineered materials and other therapies.

Ligand composition and geometry are yet more malleable biophysical cues, since they modulate adhesion and spreading of macrophages on biomaterials. BMDM cultured on laminin, Matrigel, and vitronectin all showed increased pro-healing response (measured by cytosolic arginase expression), compared to those cultured on collagen I/IV, fibronectin, or fibrinogen (Luu and Liu, 2018). However, patterning these ECMs in 20um lines significantly increased arginase expression compared to flat for collagen IV, and trended upwards for all others except vitronectin, which showed the highest arginase expression (Luu and Liu, 2018). Therefore, the physical geometry of ECM ligand presentation influences the polarization of macrophages. Some of these two-dimensional (2D) effects extend to three-dimensional (3D) biomaterial architecture. For example, photo-crosslinking of fibrin hydrogels increases spreading, motility, and inflammatory activation of BMDM perhaps by increasing the density of adhesive ligands (Hsieh et al., 2019). In contrast, 2D and 3D alginate hydrogels, both with and without RGD adhesion peptide, promote a mixed CD86+ IL-10 secreting THP-1 macrophage phenotype, compared to cells cultured on a planar tissue culture polystyrene (Delcassian et al., 2019). Thus, ligand composition and patterning are important considerations when engineering materials for macrophage modulation.

The observations above have been made in a controlled system, isolating macrophage-material interactions. In the body, these interactions occur synchronously with other cell-matrix, as well as cell-cell interactions. For example, 3T3 fibroblasts secrete more collagen when encapsulated in stiff alginate hydrogels compared to fibroblasts in soft alginate (Boddupalli and Bratlie, 2019). In coculture, myofibroblast contractions on a fibrillar collagen matrix produce significant deformation fields, which attract macrophage migration, independent of collagen fibril alignment and reproducible using micromanipulator controlled microneedles (Pakshir et al., 2019). These exchanges are interdependent and dynamic, making coculture models and in vivo testing essential to understand the impact of material properties on macrophages in a physiologic context. While in vitro experiments allow us to dissect individual interactions and pathways, in vivo work is required to put these studies in a more physiological context.

Macrophage response to biodegradable implanted biomaterials in vivo

Animal studies are a frequently used tool in the translation of basic science findings to the clinic. From skeletal support to tissue repair and replacement, the many applications of biomaterials are studied in mice, rats, swine, and hon-human primates, and utilize a wide variety of biomaterials implanted in diverse locations. These studies increase confidence in efficacy prior to first in human trials, and can also offer some insight into the role of macrophage regulation by physical and mechanical cues (Saleh and Bryant, 2017; Wermuth and Jimenez, 2015). This section describes these data, and the potential for further work (Figure 2).

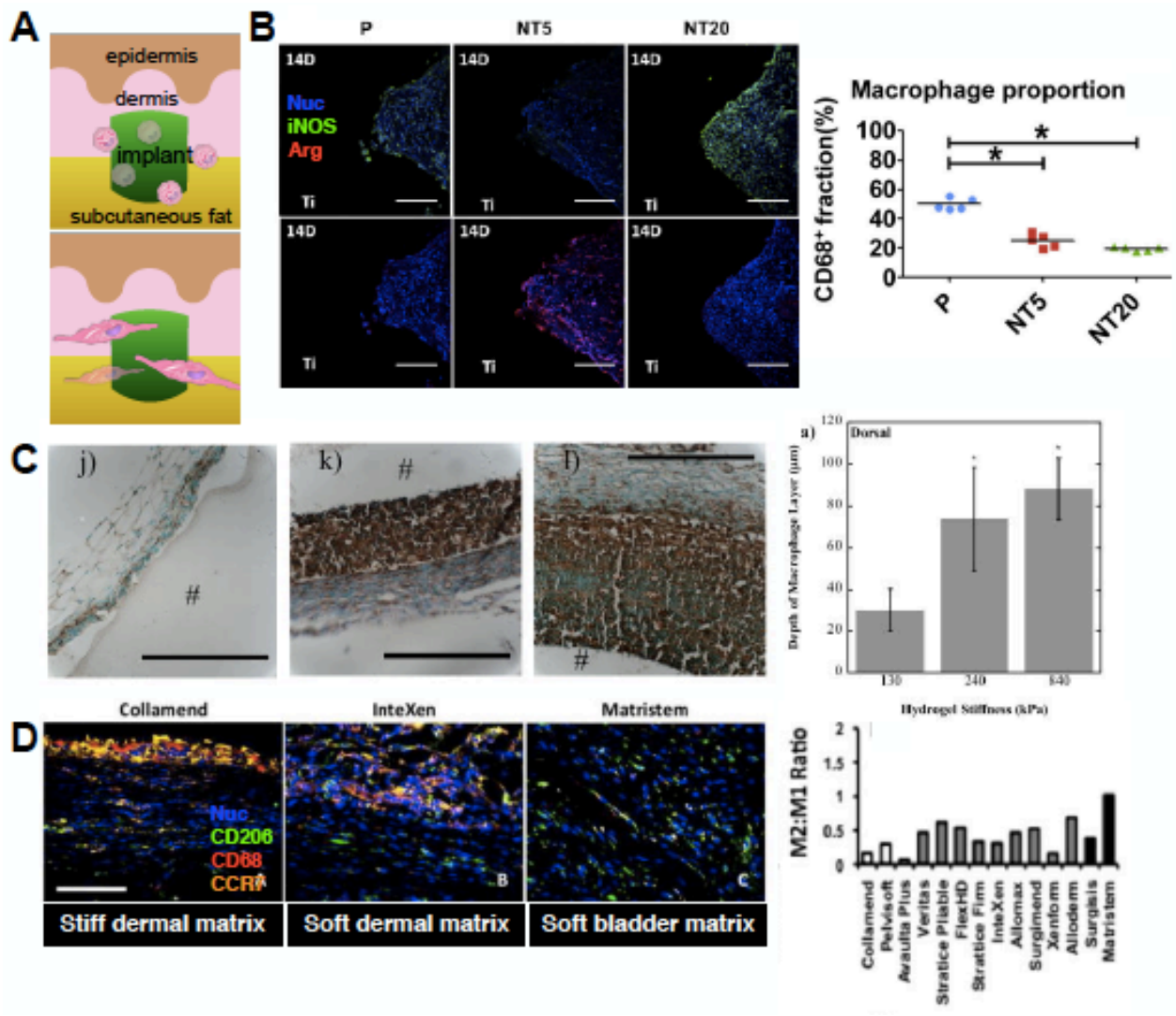

Figure 2. Effects of biophysical properties on foreign body response *in vivo*. (A) Schematic of *in vivo* studies investigating FBR. (B) Immunohistochemistry (IHC) micrographs of polished (P), moderately rough (NT5) and very rough (NT20) titanium screws implanted in rat femurs for 14 days (left) and quantification of immunohistochemistry after 7 days (right) (Ma et al., 2014). (C) Mac-3 immunohistochemistry (left) and macrophage layer quantification of subcutaneous PEG-RGD implants of varying stiffness after 28 days (Blakney et al., 2012). (D) Micrographs (left) and quantification of immunohistochemistry from subcutaneous implants of different decellularized matrices (left) (Brown et al., 2012). Figures adapted from Ma, 2014; Blakney, 2012; Brown, 2012; Smith, 2017(Smith et al., 2017).

Biodegradable hydrogels are used clinically to lend mechanical integrity to damaged tissue, occlude skin wounds, and serve as tissue replacements, and these functions may be modulated by macrophage-material interactions (Bejleri and Davis, 2019; Helary et al., 2010; Traverse et al., 2019). Both collagen and decellularized matrix materials are commercially available for clinical use, and many animal studies have explored the mechanisms by which these hydrogels regulate immune response, and thereby healing (Badylak et al., 2016; Garcia-Garcia and Martin, 2019; Sadtler et al., 2017; Sadtler et al., 2019; Witherel et al., 2016). Soft decellularized mesh composed of porcine urinary bladder matrix (UBM) promotes CD206+CD68+ anti-inflammatory macrophage infiltration and decreased fibrous capsule formation, compared to stiffer matrix mesh derived from porcine dermis (Figure 2D) (Brown et al., 2012). Stiff (322kPa) pericardium-derived collagen hydrogels have been shown to induce a transition in recruited macrophage phenotype from inflammatory to pro-healing between day 3 and day 7, in a subcutaneous implant model, while also promoting re-epithelialization of large skin wounds, compared to Tegaderm (El Masry et al., 2019). In another study, NIH Swiss nude mice with splinted full thickness excisional skin wounds showed decreased contraction with a range of dermal substitutes, including decellularized human dermal collagen matrix, bovine collagen (Integra), and polylactic-glycolic acid (PLGA) membrane functionalized with decellularized human dermal matrix (Truong et al., 2005). FBGC were found in greater numbers with Integra treatment compared to other materials, as assessed by H&E. Perhaps, although these materials are biochemically varied, their mechanical properties may help retain integrity of the wound bed, facilitating re-epithelialization and dermal proliferation and thus skin repair by regeneration, instead of contraction. Future studies may help clarify the physical cues at play in wound healing, and the cellular players that respond.

Animal studies have undoubtedly contributed to our knowledge of biophysical regulation of macrophages in various medical applications. While this platform continues to be useful for

translational studies and development of new techniques, human trials remain the ultimate test of biomaterial efficacy.

Clinical insight into the effect of physical biomaterial properties on macrophages during tissue repair.

Macrophages in tissues throughout the body respond to biophysical cues in unique ways that can be harnessed in treating injury and disease. Cell and animal studies described above have in part led to several putative macrophage modulatory materials have reached clinical testing. Here we review a case study of wound dressing materials in clinical translation that take advantage of physical immunomodulatory cues.

Restoring the physical and functional integrity of the skin after injury is a major clinical challenge, which has been made more urgent by the rising incidence of chronic wounds secondary to diabetes and peripheral vascular disease (Eming et al., 2014; Sen et al., 2009). Several matrix materials are currently being tested for use in wound therapy, including collagen-based materials and decellularized natural matrices, which are often modified with crosslinking agents to enhance mechanical properties for handling. These modifications are also likely to modulate local immune responses. Collagen hydrogels have been used extensively in the clinic to treat skin wounds (Gaspar-Pintiliescu et al., 2019; Pallaske et al., 2018); Integra is a porous hydrogel composed of bovine collagen and glycosaminoglycans, crosslinked with glutaraldehyde, resulting in a matrix with a Young's modulus of ~30 kPa (ClinicalTrials.gov, 2016a, b; Helary et al., 2010). In a prospective longitudinal study of 46 participants with diabetic foot ulcers, flowable Integra hydrogel treatment resulted in an 86.95% complete healing rate, compared to 52.17% in the control group, treated with a much stiffer (~9 MPa) saline moistened gauze dressing (Campitiello et al., 2017). A 0.4 mm version of Integra is currently in clinical trials for burn

treatment (Campitiello et al., 2017; Zhang et al., 2016). A new stiffer collagen matrix, derived from axolotl (*Ambystoma mexicanum*) dermis (Neomatrix), recently completed phase 1 clinical trials, demonstrating safety and hypoallergenic properties using a scratch test covered with an 8 mm disc for 6 hours (ClinicalTrials.gov, 2019). In another study, ten full thickness burn patients underwent split thickness autologous skin graft (STSG), in which partial thickness donor skin grafts are utilized, and wound bed preparation with Integra (~30 kPa), viscose cellulose sponge (9-12 kPa), and no material were compared side by side (Lagus et al., 2013). Punch biopsies taken 1 week after STSG showed distinct macrophage polarization: Soft cellulose sponge promoted CD163+ anti-inflammatory macrophage phenotype as well as CD31+ vessel formation, compared to stiffer Integra and control treatments over the 21 day study. Together these studies suggest that softer environments elicited by some biomaterial hydrogels promote macrophage healing phenotypes in the skin wound micro-environment through physical cues, in addition to biochemical signals.

In addition to polymeric biomaterials, decellularized tissue derived ECMs have also been explored as wound dressings (ClinicalTrials.gov, 2020). Oasis is a proprietary decellularized matrix material isolated from porcine small intestinal submucosa (SIS) and is FDA approved for many applications, including the dressing of partial and full thickness skin wounds and ulcers. Similar to Integra, Oasis hydrogels have been found to improve healing of chronic leg ulcers, when compared to stiff saline soaked gauze dressing (Mostow et al., 2005). This material also promotes the rate of complete closure in diabetic ulcers, compared to a combinatory recombinant PDGF and cellulose gel therapy (Niezgoda et al., 2005). Recently, Brown-Etris and colleagues (Brown-Etris et al., 2019) showed that Oasis treatment increases the rate of complete healing in full thickness pressure ulcers by 11%, compared to standard compression therapy alone. The unique composition of Oasis may create the synergistic biophysical and biochemical cues that govern its advantageous macrophage modulation. Studies *in vitro* show that decellularized SIS

promotes anti-inflammatory CD206 and Fizz1 expression in murine bone marrow derived macrophages, and results in lower iNOS expression, compared to decellularized matrix hydrogels from other tissues, as well as LPS/IFNγ stimulated macrophages (Dziki et al., 2017; Sicari et al., 2014). However, further studies are needed to better understand the cell-matrix interactions that govern these effects in humans, and determine whether similar effects may be observed in wound patients.

Clinical trials are the penultimate test in the application of basic science findings to treat human disease. Skin wound dressings comprise some of the most needed and life altering medical interventions, and there is still much we don't understand about how these materials interact with the host immune system. Extending the investigation of macrophage modulation to all future clinical trials of similar materials will require ingenuity, but also has the potential to define principles of material engineering and allow tuning of the immune response.

Summary

The large and growing body of data on material modulation of macrophage behavior in tissue repair is diverse and multifaceted. This variety of approaches is necessary, but consistent measures of physical properties (roughness, stiffness) and macrophage behaviors in future studies will facilitate better comparisons between data, and synthesis of consensus material engineering principles. Thus far, that the literature largely suggests that stiff substrates tend to promote an inflammatory macrophage phenotype compared to soft substrates *in vitro.* On the other hand, macrophages on rougher substrates are more amenable to adopting an anti-inflammatory phenotype, compared to those cultured on smooth surfaces, and this may play a role in improved bone integration of rough titanium implants. These effects are likely via integrins and/or ion channels on the cell surface, and intracellular mechanotransduction pathways.

Additionally, physical and biochemical properties synergize to modulation macrophage behavior, as in ligand type and geometric patterning. Animal studies enable translation of these *in vitro* findings to clinical applications, such as wound healing. In these experiments especially, consistency of readouts would enable better interpretation of trends across materials and animal models. Finally, clinical trials have studied the safety and efficacy of many immunomodulatory materials, but readouts of host immunomodulation are limited. Expanding study of explant, and indirect readouts such as peripheral blood markers may improve our understanding of material-macrophage-disease interactions, and thereby pave the way for the next generation of material therapeutics.

The work at hand

This dissertation spans in vitro and in vivo platforms, making use of the potential of each, highlighted above, to investigate targets for immunomodulation in wound healing. In Chapter 1, ECM-based gelatin methcrylate was used to assess the effects of hydrogel stiffness on full-thickness skin wound healing in mice, and explore potential mechanisms for macrophage and fibroblast mediation of these effects. Turning to in vitro platforms, Chapter 2 describes the use of 2D and 3D assays to isolate the contact-dependent effects of macrophage-fibroblast coculture on wound closure. Finally, 2D scratch closure assays and live calcium imaging of macrophages in coculture provide support for calcium-mediated mechanisms of direct macrophage-fibroblast signaling in coculture. These findings set the stage for targeted engineering of materials to enhance wound healing through immunomodulation.

References

Adlerz, K.M., Aranda-Espinoza, H., and Hayenga, H.N. (2016). Substrate elasticity regulates the behavior of human monocyte-derived macrophages. European Biophysics Journal *45*, 301-309.

Badylak, S.F., Dziki, J.L., Sicari, B.M., Ambrosio, F., and Boninger, M.L. (2016). Mechanisms by which acellular biologic scaffolds promote functional skeletal muscle restoration. Biomaterials *103*, 128-136.

Bejleri, D., and Davis, M.E. (2019). Decellularized Extracellular Matrix Materials for Cardiac Repair and Regeneration. Adv Healthc Mater *8*, e1801217.

Blakney, A.K., Swartzlander, M.D., and Bryant, S.J. (2012). The effects of substrate stiffness on the in vitro activation of macrophages and in vivo host response to poly(ethylene glycol)-based hydrogels. J Biomed Mater Res A *100*, 1375-1386.

Boddupalli, A., and Bratlie, K.M. (2019). Second harmonic generation microscopy of collagen organization in tunable, environmentally responsive alginate hydrogels. Biomaterials Science *7*, 1188-1199.

Brown, B.N., Londono, R., Tottey, S., Zhang, L., Kukla, K.A., Wolf, M.T., Daly, K.A., Reing, J.E., and Badylak, S.F. (2012). Macrophage phenotype as a predictor of constructive remodeling following the implantation of biologically derived surgical mesh materials. Acta Biomater *8*, 978-987.

Brown-Etris, M., Milne, C.T., and Hodde, J.P. (2019). An extracellular matrix graft (Oasis((R)) wound matrix) for treating full-thickness pressure ulcers: A randomized clinical trial. J Tissue Viability *28*, 21-26.

Campitiello, F., Mancone, M., Della Corte, A., Guerniero, R., and Canonico, S. (2017). To evaluate the efficacy of an acellular Flowable matrix in comparison with a wet dressing for the treatment of patients with diabetic foot ulcers: a randomized clinical trial. Updates Surg *69*, 523-529.

Cha, B.H., Shin, S.R., Leijten, J., Li, Y.C., Singh, S., Liu, J.C., Annabi, N., Abdi, R., Dokmeci, M.R., Vrana, N.E.*, et al.* (2017). Integrin-Mediated Interactions Control Macrophage Polarization in 3D Hydrogels. Adv Healthc Mater *6*.

ClinicalTrials.gov (2016a). Retrospective Study Evaluating Outcomes for Integra® Skin Sheet Products in Lower Extremity Complex Wounds (US National Library of Medicine).

ClinicalTrials.gov (2016b). A Safety and Efficacy Study of INTEGRA® Dermal Regeneration Template for the Treatment of Diabetic Foot Ulcers (US National Library of Medicine).

ClinicalTrials.gov (2019). NeoMatriX Wound Matrix Collagen Dressing Skin Prick Test (National Library of Medicine).

ClinicalTrials.gov (2020). Treatment of Wounds Using Oasis® ECM (US National Library of Medicine).

Delcassian, D., Malecka, A.A., Opoku, D., Palomares Cabeza, V., Merry, C., and Jackson, A.M. (2019). Primary human macrophages are polarized towards pro-inflammatory phenotypes in alginate hydrogels. bioRxiv, 824391.

Dziki, J.L., Wang, D.S., Pineda, C., Sicari, B.M., Rausch, T., and Badylak, S.F. (2017). Solubilized extracellular matrix bioscaffolds derived from diverse source tissues differentially influence macrophage phenotype. J Biomed Mater Res A *105*, 138-147.

El Masry, M.S., Chaffee, S., Das Ghatak, P., Mathew-Steiner, S.S., Das, A., Higuita-Castro, N., Roy, S., Anani, R.A., and Sen, C.K. (2019). Stabilized collagen matrix dressing improves wound macrophage function and epithelialization. FASEB J *33*, 2144-2155.

Eming, S.A., Martin, P., and Tomic-Canic, M. (2014). Wound repair and regeneration: mechanisms, signaling, and translation. Sci Transl Med *6*, 265sr266.

Féréol, S., Fodil, R., Labat, B., Galiacy, S., Laurent, V.M., Louis, B., Isabey, D., and Planus, E. (2006). Sensitivity of alveolar macrophages to substrate mechanical and adhesive properties. Cell Motility *63*, 321-340.

Garcia-Garcia, A., and Martin, I. (2019). Extracellular Matrices to Modulate the Innate Immune Response and Enhance Bone Healing. Front Immunol *10*, 2256.

Gaspar-Pintiliescu, A., Stanciuc, A.M., and Craciunescu, O. (2019). Natural composite dressings based on collagen, gelatin and plant bioactive compounds for wound healing: A review. International Journal of Biological Macromolecules *138*, 854-865.

Goffin, J.M., Pittet, P., Csucs, G., Lussi, J.W., Meister, J.-J., and Hinz, B. (2006). Focal adhesion size controls tension-dependent recruitment of α-smooth muscle actin to stress fibers. J Cell Biol *172*, 259-268.

Gruber, E.J., and Leifer, C.A. (2020). Molecular regulation of TLR signaling in health and disease: mechano-regulation of macrophages and TLR signaling. Innate Immun *26*, 15-25.

Hamlet, S.M., and Ivanovski, S. (2017). Inflammatory Cytokine Response to Titanium Surface Chemistry and Topography. In The Immune Response to Implanted Materials and Devices: The Impact of the Immune System on the Success of an Implant, B. Corradetti, ed. (Cham: Springer International Publishing), pp. 151-167.

Helary, C., Bataille, I., Abed, A., Illoul, C., Anglo, A., Louedec, L., Letourneur, D., Meddahi-Pelle, A., and Giraud-Guille, M.M. (2010). Concentrated collagen hydrogels as dermal substitutes. Biomaterials *31*, 481-490.

Hsieh, J.Y., Keating, M.T., Smith, T.D., Meli, V.S., Botvinick, E.L., and Liu, W.F. (2019). Matrix crosslinking enhances macrophage adhesion, migration, and inflammatory activation. APL Bioeng *3*, 016103.

Kloc, M., Ghobrial, R.M., Wosik, J., Lewicka, A., Lewicki, S., and Kubiak, J.Z. (2018). Macrophage functions in wound healing. J Tissue Eng Regen Med.

Lagus, H., Sarlomo-Rikala, M., Bohling, T., and Vuola, J. (2013). Prospective study on burns treated with Integra(R), a cellulose sponge and split thickness skin graft: comparative clinical and histological study--randomized controlled trial. Burns *39*, 1577-1587.

Leifer, C.A., Gruber, E., Stelzer, S., Erlich, E., and Sinha, S. (2016). Macrophage lipid accumulation is regulated by substrate stiffness. The Journal of Immunology *196*, 57.55.

Luu, T.U., Gott, S.C., Woo, B.W., Rao, M.P., and Liu, W.F. (2015). Micro- and Nanopatterned Topographical Cues for Regulating Macrophage Cell Shape and Phenotype. ACS Appl Mater Interfaces *7*, 28665-28672.

Luu, T.U., and Liu, W.F. (2018). Regulation of Macrophages by Extracellular Matrix Composition and Adhesion Geometry. Regenerative Engineering and Translational Medicine *4*, 238-246.

Ma, Q.L., Zhao, L.Z., Liu, R.R., Jin, B.Q., Song, W., Wang, Y., Zhang, Y.S., Chen, L.H., and Zhang, Y.M. (2014). Improved implant osseointegration of a nanostructured titanium surface via mediation of macrophage polarization. Biomaterials *35*, 9853-9867.

McWhorter, F.Y., Davis, C.T., and Liu, W.F. (2015). Physical and mechanical regulation of macrophage phenotype and function. Cell Mol Life Sci *72*, 1303-1316.

Mostow, E.N., Haraway, G.D., Dalsing, M., Hodde, J.P., King, D., and Group, O.V.U.S. (2005). Effectiveness of an extracellular matrix graft (OASIS Wound Matrix) in the treatment of chronic leg ulcers: a randomized clinical trial. J Vasc Surg *41*, 837-843.

Niezgoda, J.A., Van Gils, C.C., Frykberg, R.G., and Hodde, J.P. (2005). Randomized clinical trial comparing OASIS Wound Matrix to Regranex Gel for diabetic ulcers. Adv Skin Wound Care *18*, 258-266.

Okamoto, T., Takagi, Y., Kawamoto, E., Park, E.J., Usuda, H., Wada, K., and Shimaoka, M. (2018). Reduced substrate stiffness promotes M2-like macrophage activation and enhances peroxisome proliferator-activated receptor gamma expression. Exp Cell Res *367*, 264-273.

Pakshir, P., Alizadehgiashi, M., Wong, B., Coelho, N.M., Chen, X., Gong, Z., Shenoy, V.B., McCulloch, C.A., and Hinz, B. (2019). Dynamic fibroblast contractions attract remote macrophages in fibrillar collagen matrix. Nat Commun *10*, 1850.

Pakshir, P., and Hinz, B. (2018). The big five in fibrosis: Macrophages, myofibroblasts, matrix, mechanics, and miscommunication. Matrix Biol *68-69*, 81-93.

Pallaske, F., Pallaske, A., Herklotz, K., and Boese-Landgraf, J. (2018). The significance of collagen dressings in wound management: a review. Journal of Wound Care *27*, 692-702.

Pensalfini, M., Haertel, E., Hopf, R., Wietecha, M., Werner, S., and Mazza, E. (2018). The mechanical fingerprint of murine excisional wounds. Acta Biomater *65*, 226-236.

Previtera, M.L., and Sengupta, A. (2015). Substrate Stiffness Regulates Proinflammatory Mediator Production through TLR4 Activity in Macrophages. PLOS ONE *10*, e0145813.

Sadtler, K., Sommerfeld, S.D., Wolf, M.T., Wang, X., Majumdar, S., Chung, L., Kelkar, D.S., Pandey, A., and Elisseeff, J.H. (2017). Proteomic composition and immunomodulatory properties of urinary bladder matrix scaffolds in homeostasis and injury. Semin Immunol *29*, 14-23.

Sadtler, K., Wolf, M.T., Ganguly, S., Moad, C.A., Chung, L., Majumdar, S., Housseau, F., Pardoll, D.M., and Elisseeff, J.H. (2019). Divergent immune responses to synthetic and biological scaffolds. Biomaterials *192*, 405-415.

Sakar, M.S., Eyckmans, J., Pieters, R., Eberli, D., Nelson, B.J., and Chen, C.S. (2016). Cellular forces and matrix assembly coordinate fibrous tissue repair. Nat Commun *7*, 11036.

Saleh, L.S., and Bryant, S.J. (2017). In Vitro and In Vivo Models for Assessing the Host Response to Biomaterials. Drug Discov Today Dis Models *24*, 13-21.

Scheraga, R.G., Abraham, S., Niese, K.A., Southern, B.D., Grove, L.M., Hite, R.D., McDonald, C., Hamilton, T.A., and Olman, M.A. (2016). TRPV4 Mechanosensitive Ion Channel Regulates Lipopolysaccharide-Stimulated Macrophage Phagocytosis. J Immunol *196*, 428-436.

Sen, C.K., Gordillo, G.M., Roy, S., Kirsner, R., Lambert, L., Hunt, T.K., Gottrup, F., Gurtner, G.C., and Longaker, M.T. (2009). Human skin wounds: a major and snowballing threat to public health and the economy. Wound Repair Regen *17*, 763-771.

Sicari, B.M., Dziki, J.L., Siu, B.F., Medberry, C.J., Dearth, C.L., and Badylak, S.F. (2014). The promotion of a constructive macrophage phenotype by solubilized extracellular matrix. Biomaterials *35*, 8605-8612.

Smith, T.D., Nagalla, R.R., Chen, E.Y., and Liu, W.F. (2017). Harnessing macrophage plasticity for tissue regeneration. Adv Drug Deliv Rev.

Sommerfeld, S.D., Cherry, C., Schwab, R.M., Chung, L., Maestas, D.R., Laffont, P., Stein, J.E., Tam, A., Housseau, F., Taube, J.M*., et al.* (2019). Single cell RNA-seq in regenerative and fibrotic biomaterial environments defines new macrophage subsets. bioRxiv, 642389.

Sridharan, R., Cavanagh, B., Cameron, A.R., Kelly, D.J., and O'Brien, F.J. (2019a). Material stiffness influences the polarization state, function and migration mode of macrophages. Acta Biomater *89*, 47-59.

Sridharan, R., Ryan, E.J., Kearney, C.J., Kelly, D.J., and O'Brien, F.J. (2019b). Macrophage Polarization in Response to Collagen Scaffold Stiffness Is Dependent on Cross-Linking Agent Used To Modulate the Stiffness. ACS Biomater Sci Eng *5*, 544-552.

Traverse, J.H., Henry, T.D., Dib, N., Patel, A.N., Pepine, C., Schaer, G.L., DeQuach, J.A., Kinsey, A.M., Chamberlin, P., and Christman, K.L. (2019). First-in-Man Study of a Cardiac Extracellular Matrix Hydrogel in Early and Late Myocardial Infarction Patients. JACC Basic Transl Sci *4*, 659-669.

Truong, A.T., Kowal-Vern, A., Latenser, B.A., Wiley, D.E., and Walter, R.J. (2005). Comparison of dermal substitutes in wound healing utilizing a nude mouse model. J Burns Wounds *4*, e4.

Van Goethem, E., Poincloux, R., Gauffre, F., Maridonneau-Parini, I., and Le Cabec, V. (2010). Matrix Architecture Dictates Three-Dimensional Migration Modes of Human Macrophages: Differential Involvement of Proteases and Podosome-Like Structures. The Journal of Immunology *184*, 1049.

Wermuth, P.J., and Jimenez, S.A. (2015). The significance of macrophage polarization subtypes for animal models of tissue fibrosis and human fibrotic diseases. Clin Transl Med *4*, 2.

Witherel, C.E., Graney, P.L., Freytes, D.O., Weingarten, M.S., and Spiller, K.L. (2016). Response of human macrophages to wound matrices in vitro. Wound Repair and Regeneration *24*, 514-524.

Wong, V.W., Rustad, K.C., Akaishi, S., Sorkin, M., Glotzbach, J.P., Januszyk, M., Nelson, E.R., Levi, K., Paterno, J., Vial, I.N.*, et al.* (2011). Focal adhesion kinase links mechanical force to skin fibrosis via inflammatory signaling. Nat Med *18*, 148-152.

Wouters, O.Y., Ploeger, D.T.A., Jellema, P.P.G., de Rond, S., and Bank, R.A. (2017). Mechanobiological aspects of (dysregulated) wound healing and the foreign body response (University of Groningen.).

Zhang, P., Chen, L., Zhang, Q., and Hong, F.F. (2016). Using In situ Dynamic Cultures to Rapidly Biofabricate Fabric-Reinforced Composites of Chitosan/Bacterial Nanocellulose for Antibacterial Wound Dressings. Front Microbiol *7*, 260.

Chapter 1. Stiffness mediated immunomodulation in wound healing

Introduction

There is a large and growing need for improved clinical wound therapies (Eming et al., 2007; Sen et al., 2009). While assessing the global incidence of acute and chronic wounds remains difficult (Martinengo et al., 2019), the feasible proxy, non-infectious/non-cancerous skin and subcutaneous disease, increased over 20 percent from 2005-2015 (Kassebaum et al., 2017). Despite this trend, many aspects of wound healing remain poorly understood, including the role of key intercellular interactions. Direction of wound healing is led by immune, epithelial, and mesenchymal cell types in a dynamic matrix environment. Macrophages and fibroblasts play distinct and essential roles in wound healing. Inflammatory macrophages and their pro-healing counterparts are required for successful progression through the phases of wound healing, whereas fibroblasts generate the bulk of new wound tissue, both by cell proliferation and production of extracellular matrix (ECM) (Brazil et al., 2019; Kloc et al., 2018, 2019). Other wound effectors are also thought to be directed by macrophage secreted cytokines (Holt et al., 2010; Witherel et al., 2019; Zeng and Chen, 2010). Better understanding of cell-cell and cell-matrix interactions in during wound healing may lead to prime targets for rational design of novel treatments.

As established in the literature, wound healing requires the coordination of various cell types through multiple stereotyped phases, including: 1) coagulation/recruitment, 2) inflammation, 3)proliferation, and 4)remodeling/resolution (Boniakowski et al., 2017). The initial coagulation and recruitment phase consists primarily of immune cell recruitment, which, in conjunction with the milieu of damaged tissue, elicits the inflammatory phase. Following further cell recruitment and clearance of damaged tissue, the transition from inflammatory to proliferative phase is marked by and anti-inflammatory macrophage phenotype that, in part, facilitates expansion of the fibroblast compartment and secretion of matrix to generate new tissue in the wound bed (Eming et al.,

2014). Finally, the remodeling of this new tissue facilitates resolution of the wound, into functional tissue and/or scar. Aside from these characterized cellular and biochemical components, much of the network of interactions governing wound healing remains unexplored. This is especially true with respect to the contribution of biophysical cues.

The ECM has been shown to play multiple roles in wound healing; for example, dynamic fibroblast contractions and resulting collagen matrix deformation have been shown to attract macrophages, with the radius of deformation inversely proportional to collagen concentration (Pakshir et al., 2019). This finding implies that matrix mechanics, subject to change with remodeling or biomaterial application, may effectively modulate fibroblast-macrophage interactions. Many materials, both naturally and synthetically derived, are used in tissue engineering and regenerative medicine. Each material has different physical, chemical, and biological properties, which are often tunable in ways that can affect the material's biocompatibility. collagen, hyaluronic acid, and gelatin are examples of ECM derived materials with tunable mechanical parameters that have been shown to influence the host response (Smith et al., 2017). Just as cells sense their physical environment, cell-cell signaling may also be driven by mechanotransduction, via adhesive integrins, gap junctions, stretch-gated ion channels, and more (Gruber and Leifer, 2020; Pageon et al., 2018; Solis et al., 2019; Wouters et al., 2017). Within the scope of intercellular interactions, the role of cell-cell contact has been the road less traveled, but one that is ripe for identification of biomaterial engineering targets.

The network of cell-cell-material interactions that governs wound healing remains a functional enigma, but one that emerging technologies, such as single cell RNA sequencing (scRNAseq), have the potential to solve. In this study, full-thickness skin wound response to soft or stiff gelatin methacrylate (gelMA) hydrogel was compared to that of non-treated wounds, first by examining scar size after 30 days post-wounding (PWD30). Macrophage phenotype was then characterized using *in vitro* studies on bone marrow derived macrophages (BMDM), and by

immunohistochemistry (IHC) of wound tissue at PWD3, PWD5, and PWD10. Finally, wound cell heterogeneity and transcriptional changes with wound treatment were explored using scRNAseq of PWD5 wound tissue, where CellChat receptor-ligand network analysis of transcriptional data identified cell-cell interaction pathways modulated by wound treatment.

Methods

Gel fabrication: Lyophilized gelatin methacrylate (gelMA) (Advanced Biomatrix) was reconstituted at 20% w/v with >60C PBS; 10% Irgacure 2959 dissolved in methanol was added to gelMA to a final concentration of 0.01%. This material was kept at 37C until cast onto sterile coverslips or in situ on murine dorsal 5mm full-thickness skin wounds. GelMA stiffness was characterized by parallel plate rheometry on a DHR3 instrument (TA instruments). Briefly, 500ul of gelMA solution was pipetted onto the stage, and the 40mm plate was then lowered to 300mgap prior to 365nm UV crosslinking from below the stage. An amplitude sweep was conducted from strain of 0.01-10%, to measure storage modulus of the hydrogel. 4W 365nm UV light exposure for 1 min yielded soft 3 kPa gels, and 5 min yielded stiff 150kPa gels.

For *in vitro* experiments, 35ul thin GelMA hydrogels were cast between 18mm coverslips cured with 0.03% bind silane (95% of 95% ethanol, 0.3% 3-(Trimethoxysilyl) propylmethacrylate, 5% of 10% acetic acid), and glass slides treated with Silanization solution1. These gels were then crosslinked to achieve soft (3kPa) or stiff (150 kPa) stiffness and coverslips washed with PBS in 12-well plates prior to use for cell culture.

Cell culture: Bone marrow derived macrophages were differentiated from mouse bone marrow monocytes for 7 days in D10 media (DMEM, 10% HI-FBS, 1% Penicillin streptomycin, L-Glutamine (Gibco), 10% M-CSF L929 conditioned media). Animal studies and collection of primary cells for culture adhered to UCI IACUC protocol AUP 20-047. BMDM were seeded on GelMA hydrogel covered coverslips at 9.2e4 cells/cm^2 in D10 media and allowed to adhere for 6 hours, followed by overnight stimulation with activating cytokines LPS/IFNγ (10ng/mL each), or IL-4/IL-13 (20ng/mL each) and LPS (10ng/mL) and then collection of fixed cells, supernatant, and/or protein lysate for western blot.

ELISA: BMDM culture supernatants were collected 18hrs post stimulation for assessment of TNFα and IL-10 cytokine secretion by enzyme-linked immunosorbent assay (ELISA) following manufacturers protocol (Biolegend).

Western Blot:

Animal experiments: Animal use, husbandry, and wounding were approved by the IACUC of the University of California, Irvine. Full thickness skin wounding was carried out on p50 C57/Bl/6 mice. Mice were anesthetized using isoflurane and shaved; p50 mice were chosen to minimize the impact of hair follicles during wound healing. Dorsal skin was cleansed using 70% ethanol, and a single full thickness wound was made with 5mm biopsy punches at the dorsal midline, immediately below the scapulae. This location was chosen to minimize disruption to the wound during healing. Wounds were treated with 20ul 20% GelMA, and UV crosslinked for either 1 or 5 minutes. Wounds were then dressed with Tegaderm, followed by two ¾"x2" adhesive bandages. Mice were housed individually after wounding. Mice were monitored daily for signs of infection/healing. At 3, 5, 10, or 30 days post-wounding, mice were sacrificed and dressings carefully removed. Wounded skin was excised with a ≥5mm margin and mounted in OCT for cryosectioning or fixed in PFA overnight at 4C for whole mount imaging with dissection microscope.

Immunohistochemistry: Frozen tissue sections were thawed to room temperature and fixed in 4% PFA (Fisher) for 15 min, then washed in 4 changes of PBS (VWR). Tissues were permeabilized with 0.1% Triton-x-100 (Sigma) and then washed three times with PBS 0.1% Tween-20 (Sigma), five minutes each, before blocking in 1% BSA (MP Biomedical 0219989880) + 0.1% Tween for 2 hours. Sections immunostained with F4/80 (Thermo MF48000 BM8 1:200), Arginase (Abcam 60176 1:50), iNOS (Abcam 15323 1:100), aSMA (Abcam 5694 1:200), PDGFRa (RND AF1062 1:200) overnight 4 °C. Slides were then washed three times with PBS 0.1% Tween-

20, 10 minutes each, and then stained for 1 hour with fluorescent conjugated secondary antibodies (Thermo A21209, A21244, A21206) and Hoechst 33342 at 1:1000 dilution. After again washing three times with PBS 0.1% Tween-20, five minutes each, slides were mounted with Fluoromount (Southern Biotech) and imaged at 20x using the Olympus FV3000 laser scanning confocal microscope.

Single cell RNA sequencing: PWD5 wound tissue was dissected and then dissociated with a solution of 2.7 mg/mL collagenase, 1mpyruvate, 10 mM HEPES, in RPMI basal media.

RNA library was prepared using 10xChromium V3.1 kit, and sequenced with Novaseq on an S4 flow cell (UCI Genomic High Throughput Facility) .

Data analysis: 10xChromium sequencing Fastq output files were aligned using Cellranger, on the UCI high performance computing cluster (HPC). The resulting .tar.gz files were read into Seurat for further analysis. Data was filtered for quality control, removing cells with greater than 8% mitochondrial DNA content or greater that 8,000 genes expressed. 6 samples (3 treatment conditions in experimental duplicate) were individually normalized using SCTransform and then anchored and integrated using Seurat, with 1:50 dims.

Composite integrated data was then clustered using UMAP/PCA algorithms in Seurat followed by FindNeighbors, FindClusters functions, with parameters set at 1:15 dims, resolution 0.4. FindAllMarkers function was used to identify cluster identities by gene markers. Macrophage clusters were subset and unsupervised clustering was used to identify macrophage identities in PWD5 wound tissue. This process was repeated for fibroblasts. Macrophage and Fibroblast subsets were analyzed with FindMarkers, to characterize cluster identities and DGE between treatment conditions. Differentially expressed genes were analyzed by GO analysis in Enrichr to identify putative signaling pathways responsible for gelMA and/or stiffness-mediated changes in gene expression and thereby wound healing. CellChat cell-cell interaction network analysis was

used to characterize the effect of gelMA treatment on macrophage-fibroblast interactions. The pathways identified were then assessed for contributing receptor/ligand interactions.

Purpose	**Software**	**Version**
Sequence alignment	Cellranger	4.0
QC, clustering, DGE	Seurat	3.2.2
Platform	R	4.0.3
Visualization	ggplot	3.3.2
Data piping	dplyr	1.0.2
GO analysis	Enrichr	12.2020
Image processing	Fiji/ImageJ	2.0.0-rc-69/1.52p

Table 1. **Software used in data analysis**

Results

Soft gelMA promotes smaller scar size in murine 5mm full thickness skin wounds after 30 days of healing. To assess the effect of gelMA stiffness on scar size, compared to that of untreated wounds, 20% gelMA was crosslinked in situ on dorsal 5mm full-thickness skin wounds using 365nm light for 1min (soft, 3kPa) or 5min (stiff, 150kPa), and whole mounted tissue was collected at 30 days post wounding (PWD30) (Fig. 1A, 1B). Both soft and stiff gelMA trended towards smaller scar size, but soft gelMA showed significant reduction in scar area compared to untreated wounds (Fig. 1A, 1C). Alignment of scar along the dorsal midline (left to right in Fig. 1A) was likely due to cranio-caudal stretch in skin, with movement. Wound induced hair growth was observed, with some hairs becoming trapped beneath the scar, as seen in the non-treated whole mount image.

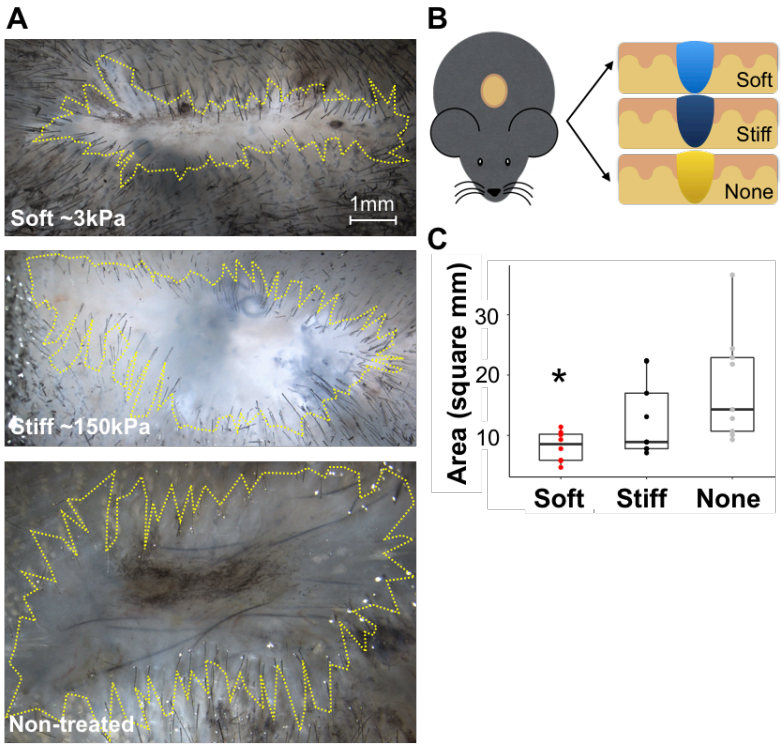

Figure 3. Soft gelMA reduces scar size at PWD30. A) Fixed, whole mounted wounds treated with soft or stiff gelMA, or no treatment, at PWD30. Scar is outlined with a yellow dashed line. B) Schematic of wounding studies for scar size at PWD30, and histology at PWD 3, 5, 10. C) Quantification of scar area from n=10 mice.

Soft gelMA promotes pro-healing phenotype in BMDM*, in vitro*. While animal studies provide a more physiologic platform to investigate cell-material interactions, in vitro studies are essential to isolate the effects of biomaterial properties from confounding variables such as other cell types, soluble factors, and native matrix. BMDM macrophages were cultured on soft or stiff gelMA or glass *in vitro* to isolate the effects of hydrogel stiffness on macrophages. BMDM seeded on soft gelMA showed more rounded morphology compared to cells on stiff gelMA and fibronectin coated glass (Fig. 2A). Upon inflammatory stimulation with LPS and IFNγ (10ng/mL each), BMDM on soft gelMA showed little inflammatory INOS expression, compared to both stiff gelMA and glass, by both immunofluorescence and Western blot (Fig. 2A, 2B). Conversely, BMDM stimulated with IL-4, IL-13, and LPS showed higher pro-healing ARG1 expression on soft gelMA compared to either stiff gelMA or glass (Fig. 2A, 2B). Interestingly, BMDM on either soft or stiff gelMA expressed a higher baseline level of arginase compared to BMDM on glass, by immunofluorescence, indicating biochemical effects of this material, in addition to the mechanically driven responses (Fig. 2A). Supernatant of these BMDM cultures at 18h after stimulation, showed a corresponding increase in TNFα and decrease in IL-10 cytokine secretion with increasing substrate stiffness (Fig. 2C, 2D). Together, these *in vitro* findings support a role for gelMA stiffness in promoting a pro-healing BMDM phenotype.

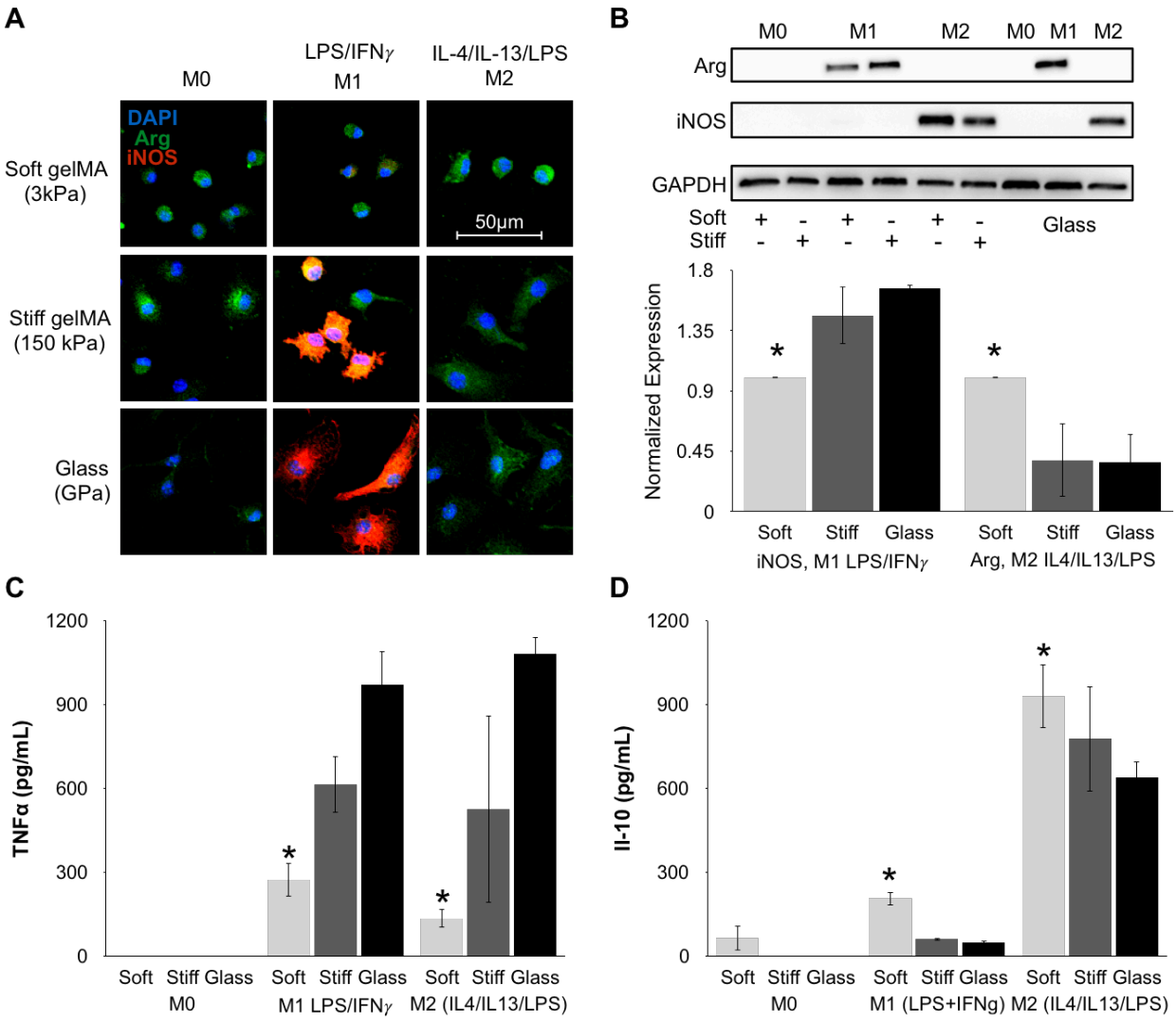

Figure 4. GelMA induces pro-healing BMDM phenotype, in vitro. A) Immunofluorescence imaging of BMDM cultured on soft or stiff gelMA, or glass, stimulated with cytokines. B) Western blots cell lysate from BMDM cultured as in A, measuring Arginase and iNOS expression, with quantification. C) Quantification of TNFa secretion from BMDM cultured as in A, after 18h stimulation. D)Quantification of IL-10 secretion from BMDM cultured as in A, after 18h stimulation.

GelMA stiffness affects macrophage recruitment and phenotype over the course of small wound healing. Wounds and surrounding skin were collected at post wound day three (PWD3), post wound day 5 (PWD5), and post wound day 10 (PWD10), across soft gelMA, stiff gelMA, and non-treated wounds for immunohistochemistry (IHC) to determine macrophage dynamics in gelMA enhanced wound healing. F4/80 positive wound macrophages were counted and phenotyped by inflammatory iNOS or pro-healing Arginase expression (Fig. 3). A lower proportion of macrophages were recruited to soft gelMA treated wounds compared to both stiff gelMA and non-treated wounds, at all time points (Fig. 3C). In contrast, the proportion of iNOS+ macrophages at PWD3 was higher in soft gelMA treated wounds than in either other treatment. This trend reversed at PWD5, and was maintained at PWD10, suggesting that soft gelMA may promote early macrophage inflammation and suppress later inflammation. Conversely, pro-healing Arg+ macrophages were increased in soft gelMA treated wounds at all-time points, compared to both soft gelMA and non-treated wounds, indicating an additional pro-healing polarization effect of this mechanically distinct hydrogel (Fig. 3C). These data support a role for therapeutic macrophage immunomodulation by gelMA stiffness during wound healing.

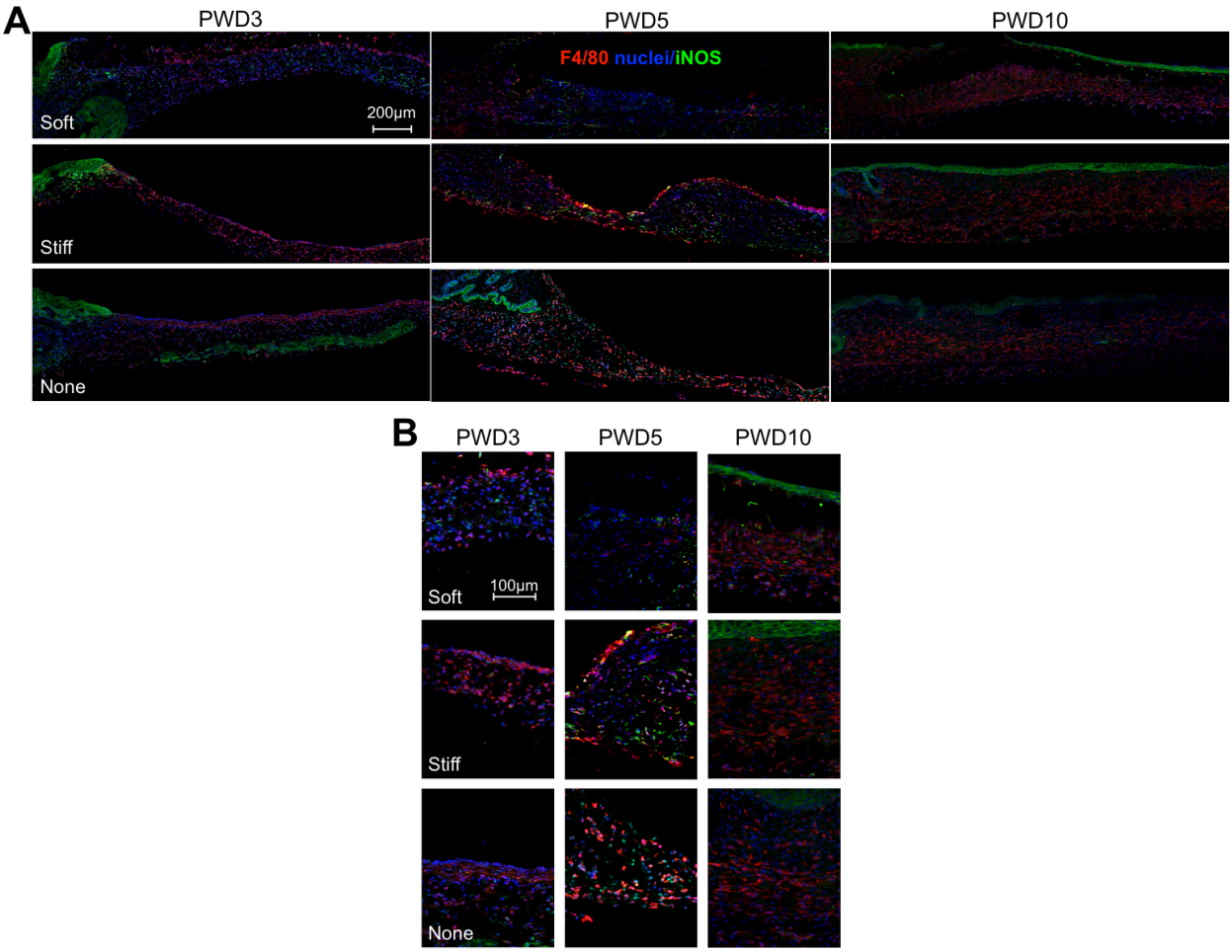

Figure 5. Temporal dynamics of macrophage phenotypes in NT, soft, stiff gelMA treated wounds. A) Immunohistochemistry of 10um sections of wound tissue at PWD3, PWD5, PWD10 across treatment groups, stained for macrophage marker F4/80, and inflammatory marker iNOS. Edge of wound is on the left, wound bed on the right. B) High magnification images of wound bed in sections from A, highlighting differences in iNOS+F4/80+ cells between treatment groups and over time.

dSingle cell RNA sequencing reveals heterogeneous and stiffness responsive macrophage and fibroblast subsets in wound tissue. To further probe the effects of gelMA and stiffness on full-thickness skin wound healing, PWD5 wound bed tissue from soft gelMA, stiff gelMA, and non-treated wounds was processed for single cell RNA sequencing. In brief, tissue from 5 mice per treatment was dissected from wound bed, excluding edges, and dissociated with collagenase, prior to single cell RNA library preparation using 10xChromium V3.1 kit. The

Novaseq platform was used to sequence an approximate 10,000 cells from each sample to 50,000 reads/cell. This study was performed in experimental duplicate, and resulting data was aligned using CellRanger and integrated and analyzed using Seurat. After quality control filters were applied, final cell numbers per wound treatment group were as follows: soft gelMA: 14,423; stiff gelMA: 16199; non-treated: 13,328; Unsupervised clustering of the composite dataset using Seurat revealed that PWD5 wound tissue contains heterogeneous immune and fibroblast populations, with multiple distinct macrophage phenotypes (Fig. 4A, 4B). Globally, 15 populations were identified with distinct gene markers highlighting putative cluster identity, such as *Birc5* in proliferating fibroblasts, and high *Col12a1* expression in contractile fibroblasts (Fig. 4A, 4C). Of these 15 clusters, 8 populations were attributed fibroblast identity via *Col1a1* expression, 3 macrophage via *Lyz2* expression, and 1 each of monocyte, dendritic cell, antigen presenting cell (APC), and T-cell groups, each identified by characteristic gene markers (Fig. 4C). This global clustering of PWD5 wound cells showed fidelity of cluster identity and potential responses to wound treatment.

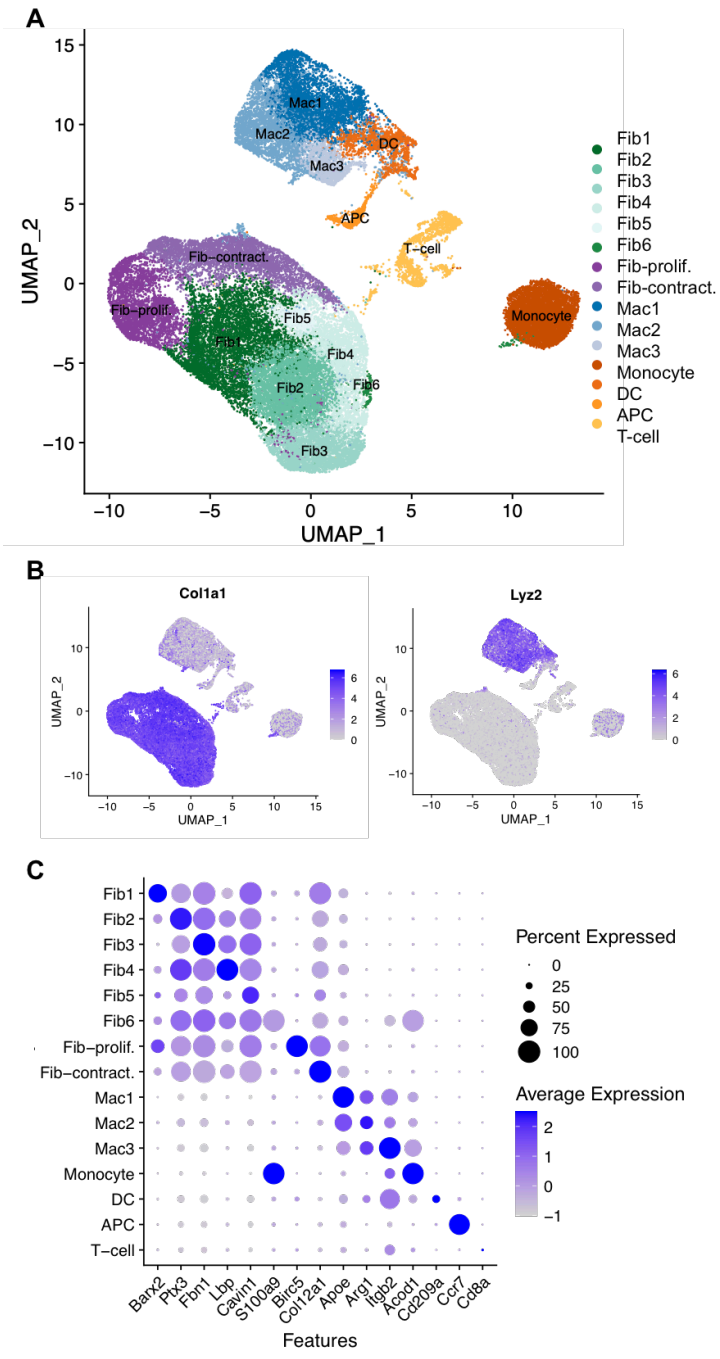

Figure 6. Fibroblast and immune wound cell populations are heterogeneous and respond to gelMA stiffness. A) UMAP plot with composite of all samples identifying 15 populations. B) Feature plots showing expression of *Col1a1* and *Lyz2*, highlighting fibroblasts and macrophages respectively. C) Relative expression of identifying genes across global wound cell populations. Size of dot indicates proportion of cells in the cluster that express the gene marker, opacity of dot indicates level of expression.

Distinct PWD5 fibroblast populations change in relative proportion and gene expression in response to wound treatment. Cells identified as fibroblasts through global clustering were subclustered using the same unsupervised Seurat function to identify populations with distinct transcriptional signatures (Fig. 5A, 5B). For example, expression of *Cenpa* distinguished Fib-DNArepair from proliferating fibroblasts, and *Lbp* was strongly upregulated in the Fib4 cluster compared to other fibroblasts (5C). In wound fibroblasts as a whole, matrix promoting *Nos2* and chemokine *Cxcl3* were upregulated with soft gelMA treatment compared to stiff gelMA and non-treated wound samples (Fig. 5D). Two of the 8 fibroblast populations also showed strong changes in relative proportion of total fibroblasts, across wound treatment groups (Fig. 5E). Fib1 comprised 26% of fibroblasts in soft gelMA treated wounds, but only 18% and 21% of stiff gelMA and non-treated wounds respectively. Conversely, Fib3 contributed only 12% of fibroblasts to soft gelMA treated wounds, in comparison to 20% and 17% of stiff gelMA and non-treated wounds respectively). All fibroblast clusters were grouped by transcriptional similarity in a cladogram, revealing a potential relationship between proliferative fibroblasts (Fib-prolif.), Fib1-Fib5, and Fib-DNArepair, and a distinction of these clusters from the contractile fibroblast cluster (Fib-contractile) and Fib5 (Fig. 5F). Relative population size and transcriptional changes in fibroblasts across wound treatments may have a complex interplay with other cell types as well.

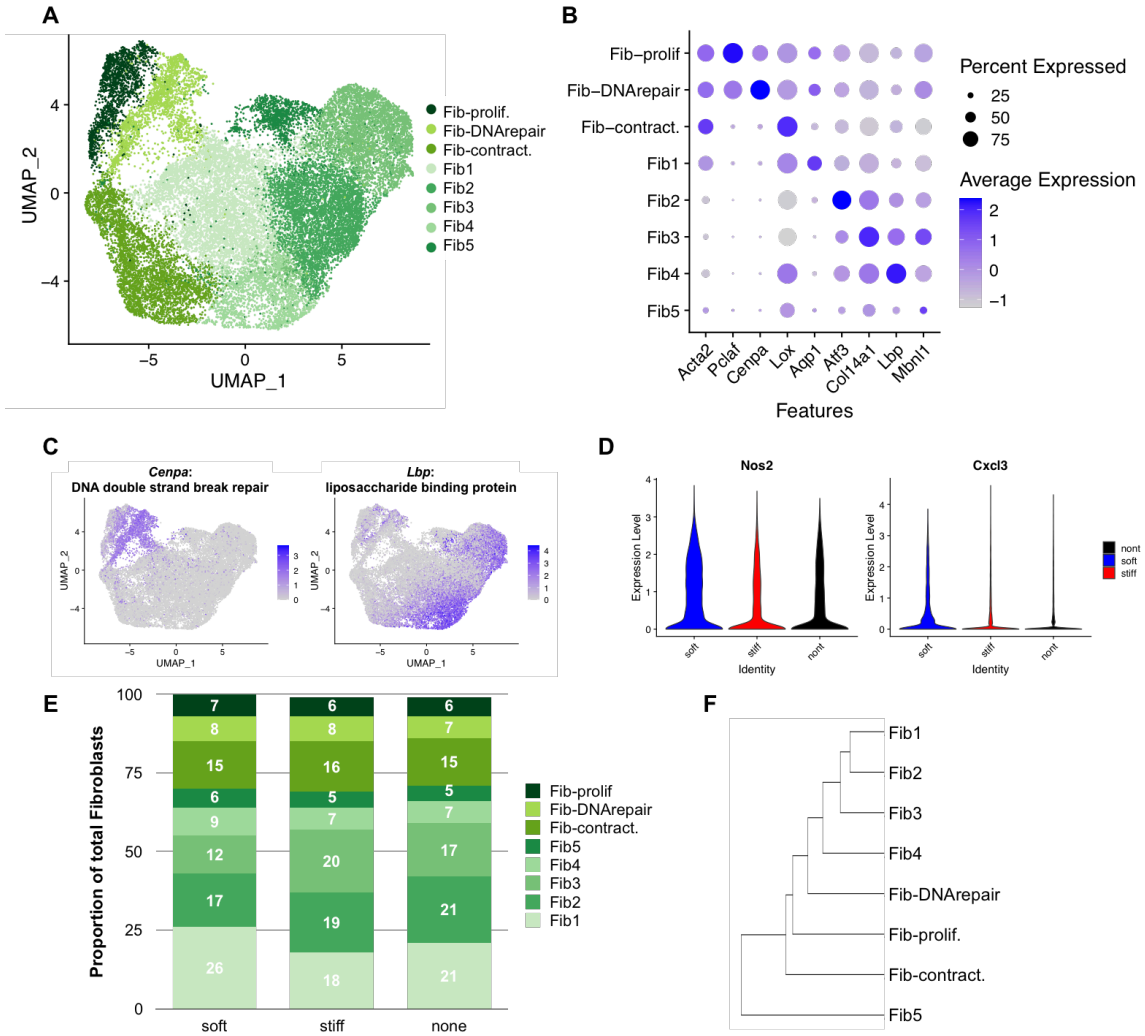

Figure 7. Heterogeneous fibroblast wound cell populations respond to gelMA stiffness. A) UMAP plot of subclustered fibroblasts, identifying 8 populations. B) Relative gene expression of identifying genes across fibroblast clusters, split by stiffness treatment. Size of dot indicates proportion of cells in the cluster that express the gene marker, color indicates treatment condition, opacity of dot indicates level of expression. C) Feature plots showing expression of *Cenpa* and *Lbp*, highlighting Fib-DNArepair and Fib4 clusters respectively. D) Violin plots comparing expression of *Nos2* and *Cxcl3* in all wound fibroblasts across wound treatments E) Stacked bar plot compares proportion of total fibroblasts held by each cluster, across stiffness treatments. F) Cladogram groups fibroblast populations by similarity of transcriptional profile.

PWD5 wound macrophages reveal population-level and calcium signaling transcriptional changes with wound treatment. Unsupervised clustering of all macrophages identified 6 populations with distinct gene expression profiles and responses to wound treatments (Fig. 6A,

6B). Notably, *Arg1* was expressed broadly across macrophage populations, except for Mac5 and Mac6, whereas *Nos2* was expressed sparsely but at high levels, primarily in the Mac3 cluster (Fig. 6C). Several genes responded to gelMA stiffness, with notably increased *Arg1* and *Ccl2* expression in soft gelMA treated wound samples, suggesting an immunosuppressive role for soft hydrogels (Fig. 6D). Additionally, the proportion of total macrophages in the Mac1 cluster comprised increased with both soft and stiff gelMA treatment, compared to non-treated wounds (Fig. 6E). The cladogram of macrophage populations suggested similar lineage for all clusters (Fig. 6F). These findings indicate potential biochemical as well as biophysical effects of gelMA treatment on wound macrophages.

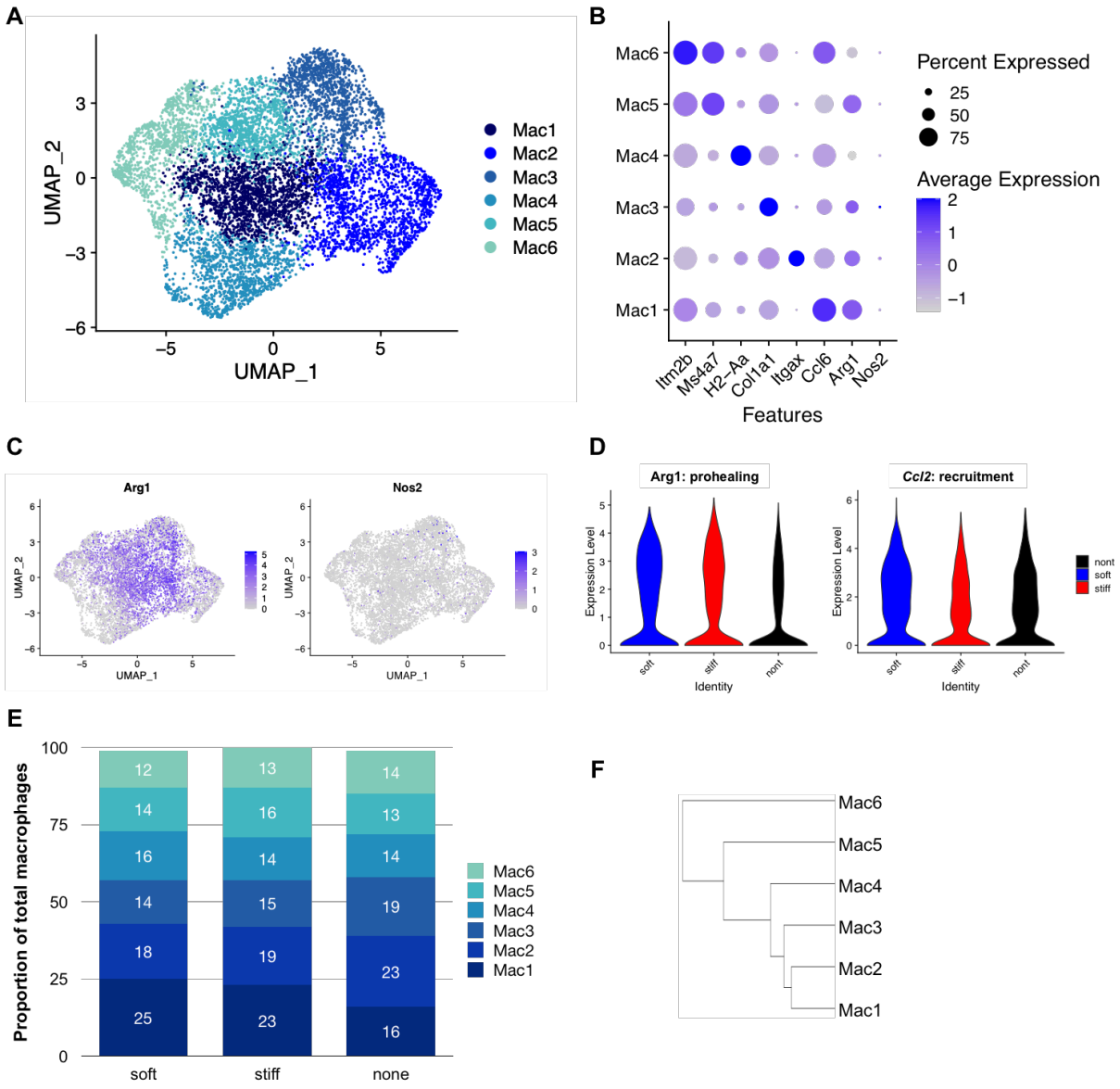

Figure 8. Heterogeneous myeloid wound cell populations respond to gelMA stiffness. A) UMAP plot of subclustered macrophages, identifying 6 populations. B) Relative gene expression of identifying genes across macrophage clusters . Size of dot indicates proportion of cells in the cluster that express the gene marker, opacity of dot indicates level of expression. C) Feature plots showing expression of S100a10 and Fbn2, highlighting Mac1 and Mac3 respectively. These populations show significant change in proportion between treatment conditions. D) violin plots of Arg1 and Ccl2 expression in all wound macrophages across wound treatments. E) Stacked bar plot compares proportion of total macrophages that contributes to each population, across stiffness treatments. F) Cladogram groups macrophage populations by similarity of transcriptional profile.

Calcium signaling related genes differentially regulated in wound macrophages and fibroblasts. Multiple genes were differentially regulated across wound treatments, especially genes associated with calcium signaling, but interestingly, growth promoting transcription factor *Egr1* was differentially regulated in macrophages and fibroblasts specifically in soft gelMA treated samples (Fig. 7). The gene was downregulated in wound fibroblasts as a whole, although both soft and stiff gelMA significantly increased the proportion of fibroblasts expressing *Egr1*. In contrast, *Egr1* was upregulated in macrophages as a whole, and expressed by a higher proportion of macrophages in the soft gelMA treated condition. These findings suggest that gelMA may have pleiotropic effects on wound effector cells, through both biochemical and biophysical interactions.

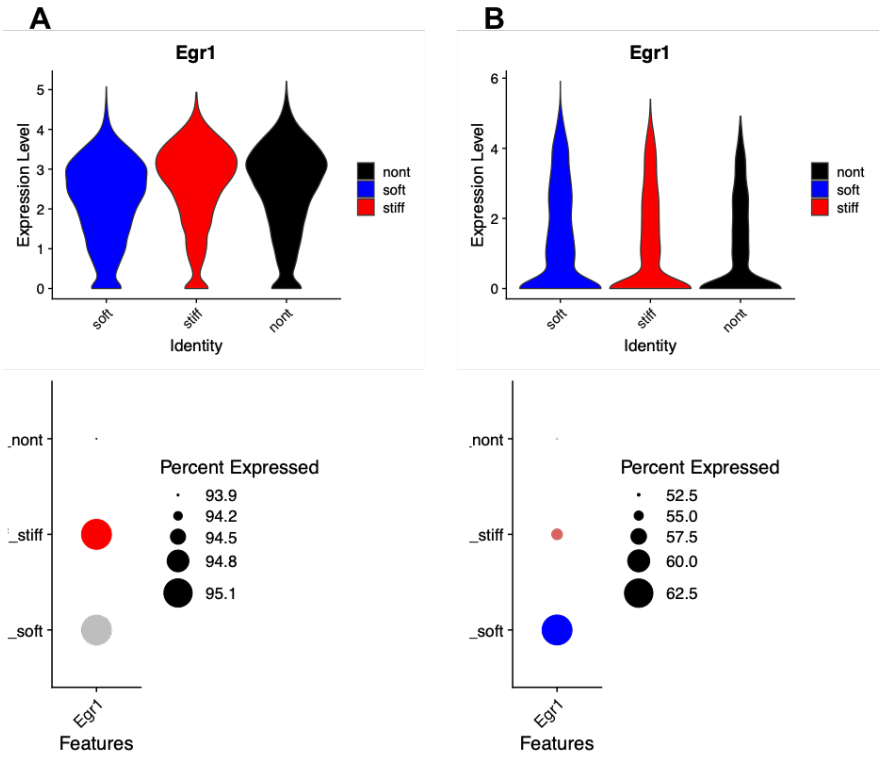

Figure 7. Soft gelMA differentially regulates calcium regulated growth promoting transcription factor *Egr1* in wound macrophages and fibroblasts. Violin and dot plots of total A) fibroblast and B) macrophage expression of *Egr1* across wound treatments.

Macrophage-fibroblast interactions may change with wound treatment. In addition to cell-material interactions, wound cells interact with neighboring cells, and this signaling may also be affected by wound treatment with gelMA. To probe this connection, macrophage and fibroblast subsets were assessed using CellChat interaction network analysis (with assistance from Dr. Christian Guerrero-Juarez in the Plikus lab). Three-way analysis revealed strong changes in the VEGF, GAS, and RANKL signaling pathways, unique to soft gelMA treatment (Fig. 7A). Pairwise analysis of soft and stiff gelMA treated samples showed upregulation of IL4 , GAS and RANKL signaling in soft gelMA treated wound cells, and stronger TNF, PTN, ANNEXIN, BMP, MK, CD137, and VEGF signaling with stiff gelMA treatment. Components of these pathways were identified as differentially regulated by wound treatment, both in fibroblast and macrophage clusters above as well as in the subsets as a whole. These findings support the complex functional regulation of wound macrophage and fibroblast subsets by stiffness of hydrogel treatment.

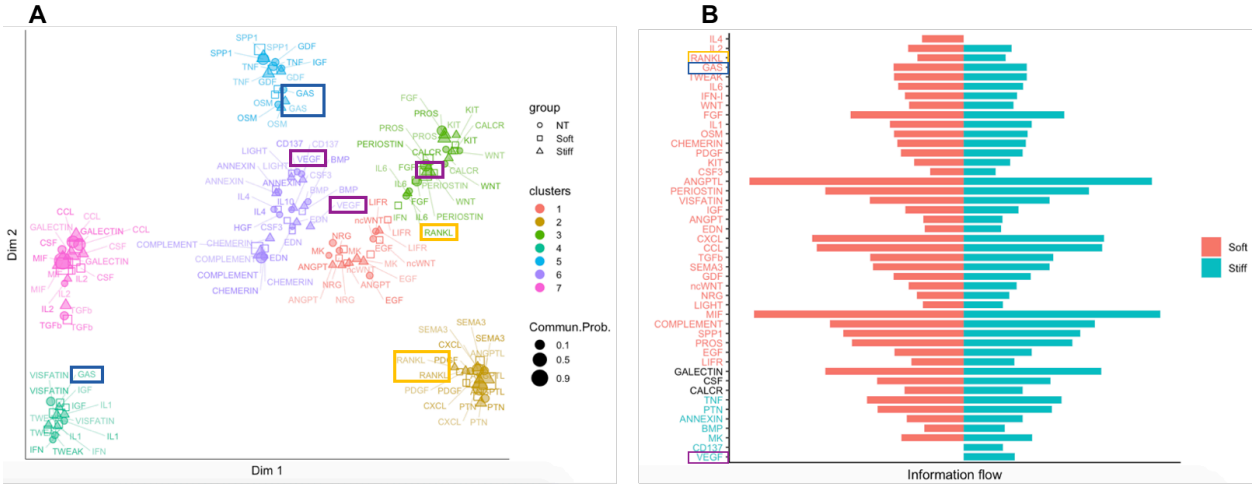

Figure 9. CellChat analysis used to identify macrophage-fibroblast interaction pathways affected by stiffness treatment. A) 2D projection of CellChat network, showing pathways grouped by similarity in strength, and function. Instances of pathways split between clusters across samples with differing treatment indicate changes in the R/L expression or source. B) Flow plot describing relative strength of tested interaction pathways in soft vs. stiff samples. Colored pathways on the Y axis are significantly difference between groups.

Discussion

In this study, soft gelMA was shown to promote a variety of favorable phenotypes, including reduced scar area of 5mm full thickness skin wounds at PWD30, and pro-healing macrophage polarization *in vitro* and *in vivo* (Fig. 1-3). Single cell RNA sequencing of PWD wound tissue revealed heterogeneous macrophage and fibroblast populations responding to wound treatment with changing proportions, and differential gene expression. Changes in macrophage gene expression highlighted the potential immunomodulatory effects of soft gelMA treatment, whereas Fib1 and Fib3 clusters altered both recruitment and matrix-related genes. Mechanistically, one common thread across macrophages and fibroblasts, was the differential regulation of genes involved in calcium signaling, indicating a potential role for this group of pathways in mechanotransduction of the wound treatment stimulus.

The in vitro and IHC phenotyping of macrophage response to gelMA stiffness followed expected trends. The rounding of macrophages on soft substrates has been observed in BMDM and other cell types, and is likely due to decreased cytoskeletal tension, compared to adhesion, as ligand density is equal in soft and stiff gelMA (Huang et al., 2012; Sridharan et al., 2019; Zhuang et al., 2020). Soft substrates have also been repeatedly shown to promote an anti-inflammatory macrophage phenotype *in vitro*, supporting the increased Arginase and IL-10 measured in BMDM on soft gelMA and re-affirmed by the increase in Arginase+F4/80+ macrophages observed by IHC in soft gelMA treated wounds at PWD3 through PWD10 (Sridharan et al., 2019; Zhuang et al., 2020). The higher resolution view afforded by scRNAseq of PWD5 wound tissue confirmed the vast complexity of wound treatment response.

In macrophages, soft gelMA notably suppressed immune activating and matrix regulatory genes, such as Il27 and endothelin receptor beta, and conversely upregulated immunoregulatory, adhesive, and selective chemotactic genes (Fig. 5). Elevation of calcium-modulated chemokine

receptor Cx3cr1 in the expanded Mac3 population aligns with published findings that transgenic knock-out of this gene results in impaired skin wound healing, driven by suppressed macrophage recruitment and resulting decreased fibroblast accumulation (Ishida et al., 2008). The increased proportion of the Mac3 cluster in soft gelMA treated wounds may indicate enhanced recruitment by this pathway, or a plastic shift of the wound macrophage population in response to the hydrogel, to facilitate fibroblast accumulation. Another upregulated calcium dependent adhesion molecule, Ceacam1, may also contribute to this effect. The In sum, these findings reveal a complex pro-healing macrophage polarization in response to soft gelMA.

In contrast to macrophage asceticism, fibroblasts responded vigorously to soft gelMA treatment, showing greater wound bed cellularity at PWD3 and PWD5 compared to stiff gelMA and non-treated wounds (Fig. 3). At the single cell level, fibroblasts modulated expression of genes that affect not only fibroblast phenotype and behavior, but also the function of the immune compartment. Fib 3 decreased in proportion with soft gelMA treatment, but put a hold on proliferation by downregulating Gas6 and upregulating tumor suppressor Edn1, both of which are calcium dependent. This cluster also downregulated matrix component Col14a, and muted the type II immune response but suppressing Saa1. The downregulation of hair follicle growth associated Bmp2 is difficult to interpret, and may be a temporal artifact or a marker of efficiency, as small wounds in mice typically heal by contraction and not regeneration (Su et al., 2009). proliferation. In contrast, the expanded Fib 1 cluster upregulated immunoregulatory Il4, which is also associated with suppression of critical fibronectin production after wounding, indicating that perhaps soft gelMA provides negative feedback on secretion of additional matrix (Serezani et al., 2017). This strong and diverse transcriptional regulation of fibroblasts effected by soft gelMA emphasizes the interplay of cell-matrix and cell-cell interactions

Many of the genes differentially regulated by soft gelMA in comparison to stiff gelMA and non-treated samples are associated with calcium-dependent signaling. Calcium regulation

induces diverse effects across many cell types, and notably may facilitate mechanotransduction. For example, Aqp1 has been shown to induce water flux driven activation of mechanosensitive ion channels by membrane stretch, and downregulation in Fib1 may curtail that response (Agbani et al., 2018). Conversely, Edn downregulation in Fib3 may be compounded by the parallel downregulation of Ednrb in Mac1. Some enigmas remain, such as the Downregulation of Cx3cr1 in fibroblasts and concomitant upregulation of the same gene in macrophages. The pleiotropic roles of calcium signaling and other pathways in immune and stromal cells make understanding their combinatorial effects that much more important to developing biomaterial engineering targets for future wound therapies.

Future work

Apply unbiased analysis to the scRNAseq dataset to assess the effects of gelMA stiffness on transcription factors, ECM regulation, YAP targets, mechanosensitive targets, adhesome targets, and more. Generate index or network of mechanically regulated genes and evaluate the score across wound treatments.

Evaluate the relative contribution of R/L pairs in the differentially regulated interaction pathways identified by CellChat.

Validate targets identified by scRNAseq using RNAscope, IHC, or KO cell/animal studies.

Examine transcriptional changes over the course of wound healing to determine if soft gelMA accelerates wound healing, or truly changes the process through biophysical signaling.

References

Agbani, E.O., Williams, C.M., Li, Y., van den Bosch, M.T., Moore, S.F., Mauroux, A., Hodgson, L., Verkman, A.S., Hers, I., and Poole, A.W. (2018). Aquaporin-1 regulates platelet procoagulant membrane dynamics and in vivo thrombosis. JCI Insight *3*.

Boniakowski, A.E., Kimball, A.S., Jacobs, B.N., Kunkel, S.L., and Gallagher, K.A. (2017). Macrophage-Mediated Inflammation in Normal and Diabetic Wound Healing. J Immunol *199*, 17-24.

Brazil, J.C., Quiros, M., Nusrat, A., and Parkos, C.A. (2019). Innate immune cell-epithelial crosstalk during wound repair. J Clin Invest *129*, 2983-2993.

Eming, S.A., Krieg, T., and Davidson, J.M. (2007). Inflammation in wound repair: molecular and cellular mechanisms. J Invest Dermatol *127*, 514-525.

Eming, S.A., Martin, P., and Tomic-Canic, M. (2014). Wound repair and regeneration: mechanisms, signaling, and translation. Sci Transl Med *6*, 265sr266.

Gruber, E.J., and Leifer, C.A. (2020). Molecular regulation of TLR signaling in health and disease: mechano-regulation of macrophages and TLR signaling. Innate Immun *26*, 15-25.

Holt, D.J., Chamberlain, L.M., and Grainger, D.W. (2010). Cell–cell signaling in co-cultures of macrophages and fibroblasts. Biomaterials *31*, 9382-9394.

Huang, X., Yang, N., Fiore, V.F., Barker, T.H., Sun, Y., Morris, S.W., Ding, Q., Thannickal, V.J., and Zhou, Y. (2012). Matrix stiffness-induced myofibroblast differentiation is mediated by intrinsic mechanotransduction. Am J Respir Cell Mol Biol *47*, 340-348.

Ishida, Y., Gao, J.L., and Murphy, P.M. (2008). Chemokine receptor CX3CR1 mediates skin wound healing by promoting macrophage and fibroblast accumulation and function. J Immunol *180*, 569-579.

Kassebaum, N.J., Smith, A.G.C., Bernabe, E., Fleming, T.D., Reynolds, A.E., Vos, T., Murray, C.J.L., Marcenes, W., and Collaborators, G.B.D.O.H. (2017). Global, Regional, and National Prevalence, Incidence, and Disability-Adjusted Life Years for Oral Conditions for 195 Countries, 1990-2015: A Systematic Analysis for the Global Burden of Diseases, Injuries, and Risk Factors. J Dent Res *96*, 380-387.

Kloc, M., Ghobrial, R.M., Wosik, J., Lewicka, A., Lewicki, S., and Kubiak, J.Z. (2018). Macrophage functions in wound healing. J Tissue Eng Regen Med.

Kloc, M., Ghobrial, R.M., Wosik, J., Lewicka, A., Lewicki, S., and Kubiak, J.Z. (2019). Macrophage functions in wound healing. J Tissue Eng Regen Med *13*, 99-109.

Martinengo, L., Olsson, M., Bajpai, R., Soljak, M., Upton, Z., Schmidtchen, A., Car, J., and Jarbrink, K. (2019). Prevalence of chronic wounds in the general population: systematic review and meta-analysis of observational studies. Ann Epidemiol *29*, 8-15.

Pageon, S.V., Govendir, M.A., Kempe, D., and Biro, M. (2018). Mechanoimmunology: molecular-scale forces govern immune cell functions. Mol Biol Cell *29*, 1919-1926.

Pakshir, P., Alizadehgiashi, M., Wong, B., Coelho, N.M., Chen, X., Gong, Z., Shenoy, V.B., McCulloch, C.A., and Hinz, B. (2019). Dynamic fibroblast contractions attract remote macrophages in fibrillar collagen matrix. Nat Commun *10*, 1850.

Sen, C.K., Gordillo, G.M., Roy, S., Kirsner, R., Lambert, L., Hunt, T.K., Gottrup, F., Gurtner, G.C., and Longaker, M.T. (2009). Human skin wounds: a major and snowballing threat to public health and the economy. Wound Repair Regen *17*, 763-771.

Serezani, A.P.M., Bozdogan, G., Sehra, S., Walsh, D., Krishnamurthy, P., Sierra Potchanant, E.A., Nalepa, G., Goenka, S., Turner, M.J., Spandau, D.F.*, et al.* (2017). IL-4 impairs wound healing potential in the skin by repressing fibronectin expression. J Allergy Clin Immunol *139*, 142-151 e145.

Smith, T.D., Nagalla, R.R., Chen, E.Y., and Liu, W.F. (2017). Harnessing macrophage plasticity for tissue regeneration. Adv Drug Deliv Rev.

Solis, A.G., Bielecki, P., Steach, H.R., Sharma, L., Harman, C.C.D., Yun, S., de Zoete, M.R., Warnock, J.N., To, S.D.F., York, A.G.*, et al.* (2019). Mechanosensation of cyclical force by PIEZO1 is essential for innate immunity. Nature *573*, 69-74.

Sridharan, R., Cavanagh, B., Cameron, A.R., Kelly, D.J., and O'Brien, F.J. (2019). Material stiffness influences the polarization state, function and migration mode of macrophages. Acta Biomater *89*, 47-59.

Su, R., Zhang, W.G., Sharma, R., Chang, Z.L., Yin, J., and Li, J.Q. (2009). Characterization of BMP2 gene expression in embryonic and adult Inner Mongolia Cashmere goat (Capra hircus) hair follicles. Canadian Journal of Animal Science *89*, 457-462.

Witherel, C.E., Abebayehu, D., Barker, T.H., and Spiller, K.L. (2019). Macrophage and Fibroblast Interactions in Biomaterial-Mediated Fibrosis. Adv Healthc Mater *8*, e1801451.

Wouters, O.Y., Ploeger, D.T.A., Jellema, P.P.G., de Rond, S., and Bank, R.A. (2017). Mechanobiological aspects of (dysregulated) wound healing and the foreign body response (University of Groningen.).

Zeng, Q., and Chen, W. (2010). The functional behavior of a macrophage/fibroblast co-culture model derived from normal and diabetic mice with a marine gelatin-oxidized alginate hydrogel. Biomaterials *31*, 5772-5781.

Zhuang, Z., Zhang, Y., Sun, S., Li, Q., Chen, K., An, C., Wang, L., van den Beucken, J.J.J.P., and Wang, H. (2020). Control of matrix stiffness using methacrylate-gelatin hydrogels for macrophage-mediated inflammatory response. ACS Biomater Sci Eng.

Chapter 2. Macrophages and fibroblasts exert reciprocal, contact-dependent effects during *in vitro* wound closure

Abstract

Wound healing involves the orchestrated communication and activities of many different cell types. Fibroblasts migrate and generate contractile forces to mediate wound closure, and remodel the extracellular matrix in healing tissue. Concurrently, macrophages coordinate many aspects of the inflammatory and healing processes, responding dynamically to changes in their local physical and biochemical environment. In this study, the reciprocal effects of macrophages and fibroblasts were examined using 2D and 3D wound closure assays. Coculture of murine bone marrow derived macrophages with 3T3 fibroblasts significantly enhanced fibroblast closure of 2D and 3D scratch wounds, and altered macrophage activation, when compared to culture of ether cell type alone. Interestingly, enhanced closure was only observed when macrophages and fibroblasts were cultured in direct contact; separation using a transwell system abrogated the effect. In direct coculture, macrophages responded to the presence of fibroblasts with increased IL-10 secretion and suppressed Tnfα secretion, in response to activating cytokines. In transwell coculture, macrophages also showed suppressed Tnfα expression but no change in IL-10 compared to monoculture. Finally, broad inhibition of gap junctions with palmitoleic acid abrogated fibroblast enhanced macrophage IL-10 secretion, suggesting that cell-cell contact through gap junctions may, in part, mediate macrophage-fibroblast communication. This work demonstrates a critical role for direct macrophage-fibroblast interactions in cellular wound healing, and reveals the potential for molecular targeting in wound healing therapeutics.

Introduction

Wound healing is a complex, dynamic process, and a better fundamental understanding remains a bottleneck in the pipeline to fulfill the growing need for new therapies (Eming et al., 2014; Kassebaum et al., 2017; Martinengo et al., 2019; Sen et al., 2009). Macrophages and fibroblasts, in particular, play distinct and essential roles during wound healing. Both inflammatory macrophages and their pro-healing counterparts are required to mediate successful transitions through multiple phases of injury response, while fibroblasts in the wound bed generate the bulk of new wound tissue and differentiate into contractile myofibroblasts, facilitating wound closure (Boddupalli et al., 2016; Boniakowski et al., 2017; Glaros et al., 2009; Wong et al., 2013). Signaling molecules produced by activated macrophages are known to affect fibroblast behavior, and visa versa, but these interactions have yet to be isolated and characterized mechanistically, and previous in vitro studies comparing macrophage and fibroblast secreted cytokines and morphology in coculture have found conflicting trends. (Holt et al., 2010; O'Rourke et al., 2019; Witherel et al., 2019). Furthermore, both macrophages and fibroblasts are also thought to direct a variety of other wound effectors, such as keratinocytes and endothelial cells, through secreted cytokines and matrix, and thus may hold promise as targets for wound treatments (Brazil et al., 2019; Kloc et al., 2019). While these and other major cellular and biochemical players in the wound healing process have been characterized, reciprocal biophysical interactions between wound effector cells, and corresponding governing mechanisms, remain poorly understood.

There are many factors that mediate macrophage-fibroblast interactions, including the wound microenvironment, other cell types, and composition of bordering tissue (Brazil et al., 2019). The complexity of the in vivo environment can make it difficult to uncover mechanisms underpinning observed behavior at the cell, tissue, and even organ level. Controlled *in vitro* systems provide a platform to tease apart these details, with high-throughput modular assays that can be sampled at multiple time points. For example, Sakar and colleagues (Sakar et al., 2016),

used a 3D fibroblast-collagen microtissue platform to isolate and identify the greater contribution of fibroblast contraction to wound closure, compared to migration into newly secreted matrix. The use of in vitro 2D and 3D wound assays, with control of geometry, cell type and number, holds further potential for the investigation of specific cell-cell and cell-matrix interactions and cellular responses.

Fibroblasts and macrophages are essential to wound healing, and their interactions play a crucial and relatively unexplored role in this process. In this study, coculture with BMDM was found to increase 3T3 scratch closure in 2D, and this effect is contact dependent. Fibroblast coculture suppressed BMDM Tnfα secretion independent of cell-cell contact, and promoted IL-10 production in a contact dependent manner. These reciprocal effects extended to 3D culture suspended in a collagen hydrogel, where BMDM also promoted 3T3 closure of puncture wounds, and 3T3 modulated BMDM to a pro-healing phenotype. Finally, gap junctions were identified as one potential mechanism for contact-dependent effects of fibroblasts on BMDM.

Methods

Cell Culture: NIH 3T3 fibroblasts were cultured at below 85% confluence in DMEM complete media (DMEM+glucose+pyruvate+Gln (Corning), 10% HI-FBS (Gibco), 1% Penicillin streptomycin, L-Glutamine (Gibco)) and used at passage 3-12. For 2D coculture experiments, 3T3 were stained with DiO or DiI membrane stain (Fisher, 5uL/mL) for 40 min in DMEM basal media at 37 C and washed twice with DMEM complete before use. Bone marrow derived macrophages were derived from mouse bone marrow cells, differentiated for 7 days in D10 media (DMEM, 10% HI-FBS, 1% Penicillin streptomycin, L-Glutamine (Gibco), 10% M-CSF L929 conditioned media). Fluorescently labelled BMDM were derived from LysMCre TdTomato$^{fl/+}$ mice, courtesy the Plikus lab. Collection of primary cells for culture adhered to institutional IACUC protocol AUP 20-047.

2D Scratch assay and coculture**:** Membrane labelled 3T3 fibroblasts in DMEM complete media were seeded at 7.9e4 cells/cm^2 in a fibronectin (10ug/mL) coated 24-well polystyrene well plate and allowed to adhere for 3 hours. For coculture conditions, BMDM were suspended in DMEM complete and seeded either on top of the 3T3 monolayer (juxtacrine) or into a 0.3um pore transwell insert (paracrine) at varying densities. After allowing adhesion for an additional 4 hours, cultures were stimulated with activating cytokines overnight (LPS/IFNγ 10ng/mL, or IL-4/IL-13 20ng/mL +LPS 10ng/mL (Fisher, R&D systems, Biolegend)). Subsequently, vertical scratches were made, one per well, using a 10ul pipette tip, and cultures were imaged at 0h and 6h following scratch, using the 4x objective on an Olympus inverted fluorescence microscope. Thymidine (2mM, Sigma) was used to inhibit proliferation during scratch closure. Area of scratch in paired single frames was measured at 0h and 6h, in triplicate per condition, and the difference in area between time points was designated area closed.

3D Wounding assay: 1mm thick collagen gels (2 or 8 mg/mL, Corning) were prepared according to manufacturer specifications, using DMEM basal media as the solvent and with the addition of 1e6 3T3/mL with or without 1e6 BMDM/mL. Gels were cast in 6-well or 12-well polystyrene plates, gelled for 30 min at 37C, then hydrated with DMEM complete media and incubated at 37C 5% CO2. After 48h, gels were wounded and imaged, using calcein AM (Fisher) or cell tracker green (CMFDA, Fisher) to visualize live cell bodies. Gels were washed and re-hydrated with DMEM complete after imaging, and placed at 37C incubation once again. After a further 72h, gels were imaged again to determine percent wound closure.

Cytokine Quantification**:** Biolegend ELISA kits for mouse IL-10 and Tnfα were used to determine concentrations of these cytokines in the supernatant, collected 6h after scratch, and were used as directed by the manufacturer.

Results

Bone marrow derived macrophages (BMDM) enhance 3T3 fibroblast scratch wound closure. Cocultures were prepared by sequentially seeding fibroblasts and varying amounts of BMDM on fibronectin coated 24-well plates, as shown in Figure 1A. These cultures were incubated overnight with DMEM complete media, inflammatory cytokines LPS+IFNγ, or pro-healing cytokines IL-4+IL-13+LPS, and monolayers were then scratched and imaged at 0h and 6h to assess closure (Fig.1A, 1B). The addition of BMDM significantly increased scratch closure at both a 1:1 and 2:1 (fibroblast : BMDM) ratio, compared to 3T3 alone, across all stimulation conditions (Fig. 1C).

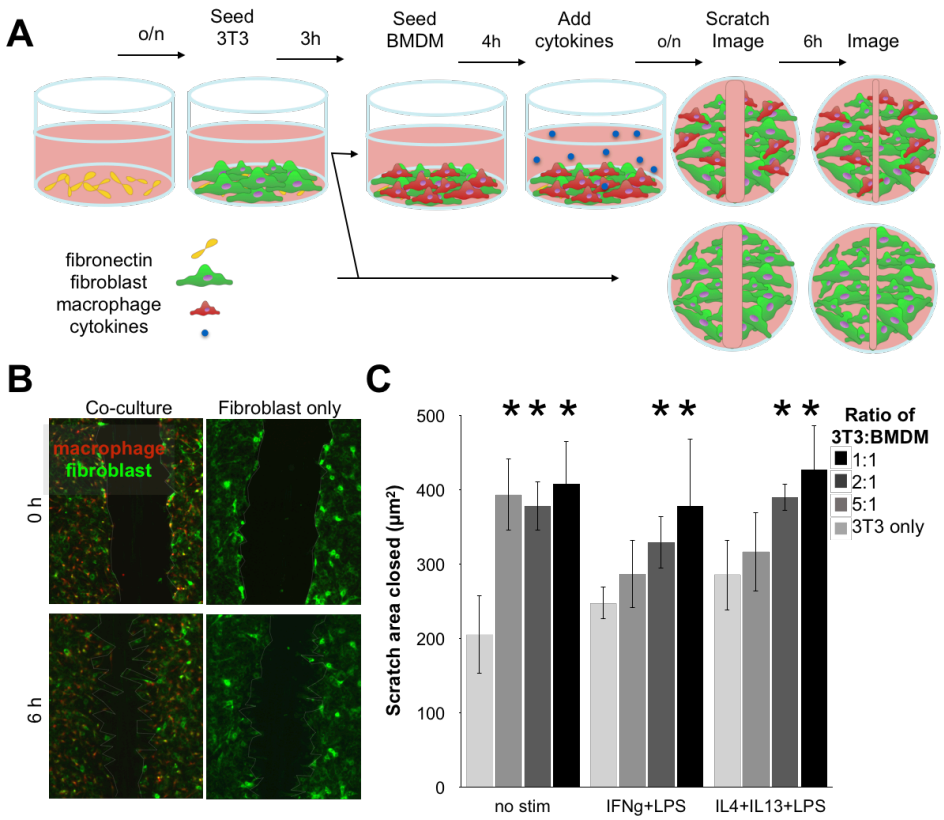

Figure 1. Juxtacrine BMDM coculture improves scratch wound closure, compared to 3T3 fibroblasts alone. A) Schematic of 2D coculture scratch experiments. B) Fluorescence micrographs of DiO stained 3T3 scratch closure over 6 hours, in the presence or absence of tdTomato expressing BMDM in a 1:1 ratio. C) Quantification of 3T3 scratch closure in the presence of varying proportions of BMDM, in the presence or absence of stimulating cytokines (LPS/IFNγ 10ng/mL, IL-4/IL13 20ng/mL). *indicates $p<0.05$ with student's t-test, compared to 3T3 only with same cytokine stimulation.

Scratch closure of 3T3 monocultures was independent of cell density, proliferation, and secreted factors, providing further evidence that the effects of BMDM are mediated biophysical interactions and not by differences in cell number (Fig. 2). Further, in conditions stimulated with inflammatory or pro-healing cytokines, scratch closure was enhanced in proportion to the added number of BMDM (Fig. 1C). However, cocultures without stimulation showed strong, uniform enhancement of scratch closure with the addition of BMDM at any ratio. Together, these data show significantly increased fibroblast scratch wound closure with macrophage coculture.

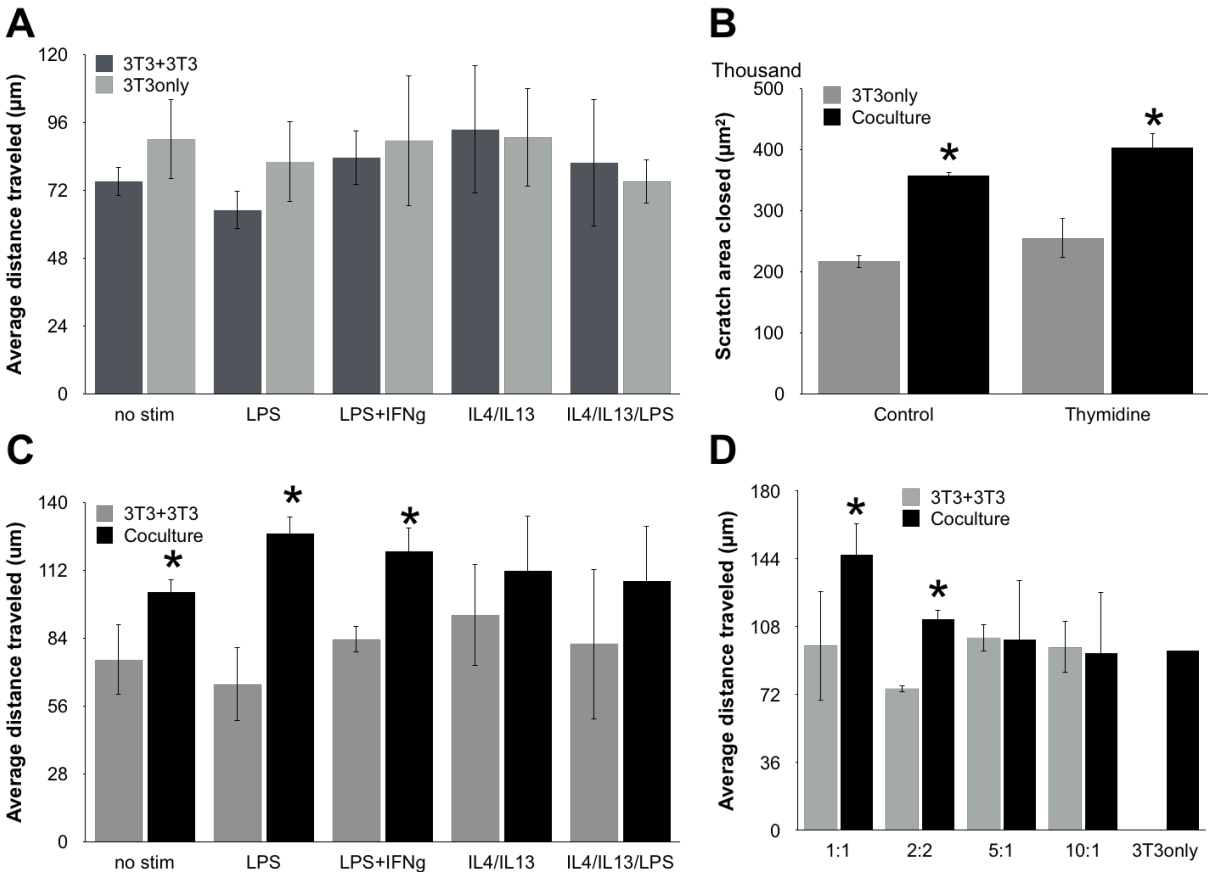

Figure 2. Scratch closure is similar regardless of 3T3 density, and independent of proliferation and fibronectin coating. Quantification of scratch closure of DiO stained 3T3 monoculture, A) with or without the addition of 1:1 unstained 3T3 after 3h, B) with or without addition of 1:1 unstained BMDM, in the presence or absence of cell cycle inhibitor thymidine, C) with or without the addition of 1:1 BMDM after 3h. Cocultures were stimulated with indicated cytokines 4h after BMDM seeding, or D) with varying ratios of BMDM:3T3 coculture.

Macrophage enhanced scratch closure is contact dependent. To test the contact dependence of BMDM-enhanced 3T3 scratch wound healing, transwell inserts were used to establish dynamic paracrine coculture with BMDM and 3T3 in a multiwell plate (Fig. 3A). Due to the constraint of transwell surface area, paracrine coculture experiments and respective controls were conducted with 5:1 (3T3 : BMDM) ratio. Coculture of BMDM and 3T3s in transwell configuration, in which only paracrine signaling was allowed, did not increase closure compared to 3T3 alone, in contrast to the juxtacrine coculture enhanced closure (Fig. 3B, 1C). The addition of BMDM conditioned media also had no effect on 3T3 scratch closure (Fig. 3C). Transwell

cocultures stimulated with LPS/IFNγ or LPS/IL-4/IL-13 also showed no BMDM-mediated scratch enhancement, consistent with what was observed in juxtacrine culture (Fig. 1C, 2D, 3B). Thus, contact with unactivated macrophages may be required to promote fibroblast scratch wound closure.

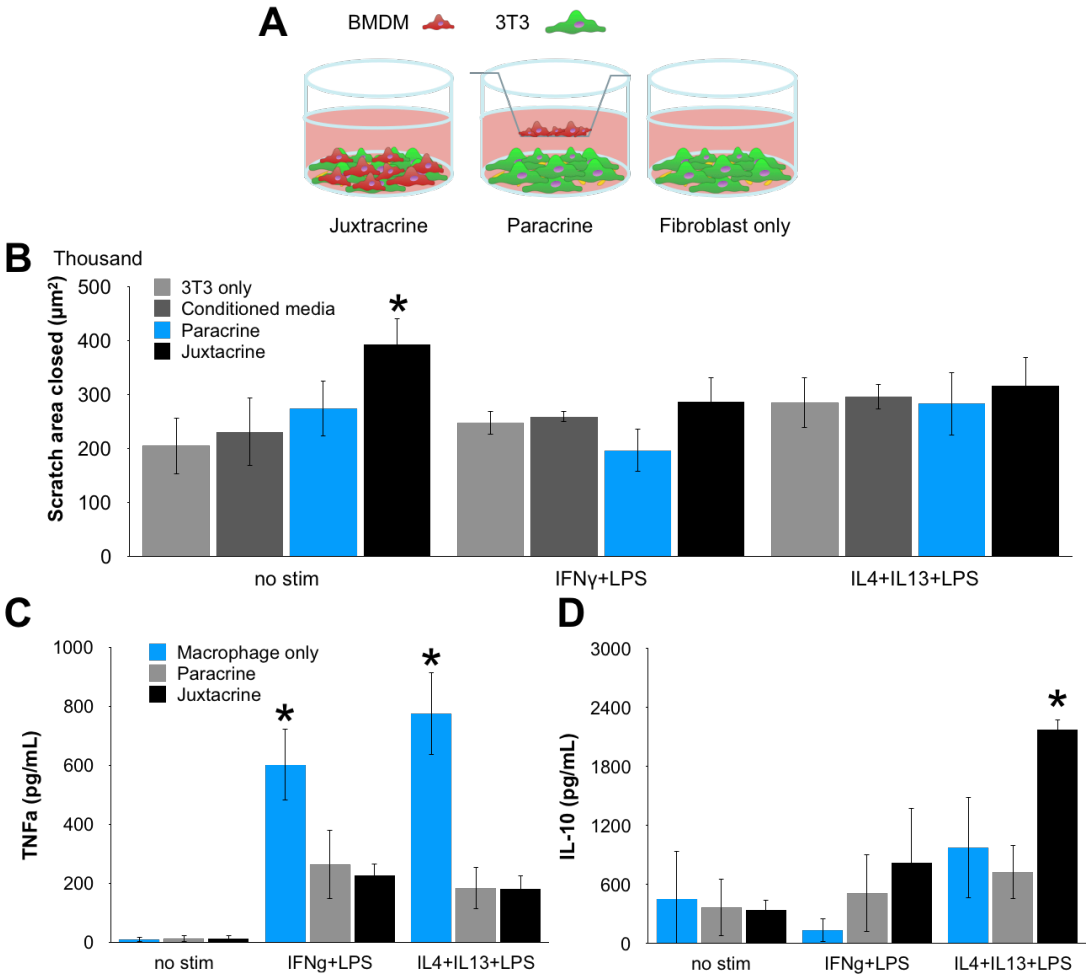

Figure 3. BMDM enhanced scratch closure is contact dependent; cytokine secretion is more complex. A) Schematic of juxtacrine vs. paracrine vs. monoculture experimental setup. B) Quantification of 3T3 scratch closure over 6 hours, in monoculture (gray), 5:1 juxtacrine (black) or 5:1 paracrine (blue) BMDM coculture, or conditioned media (dark grey). C-D) Secretion of C) TNFa or D) IL-10 in coculture conditions described in A, and BMDM only (gray). *indicates $p<0.05$ with student's t-test, compared to 3T3 only with same cytokine stimulation.

Fibroblasts affect BMDM activation. Coculture also revealed a converse relationship, the influence of 3T3 fibroblasts on macrophage cytokine secretion in response to stimulation. Cytokines in cell culture supernatant, measured using ELISA showed that 3T3 coculture enhanced LPS/IL4/IL14-induced IL-10 production in juxtacrine coculture, but not paracrine coculture. On the other hand, 3T3s suppressed LPS/IFNγ-induced Tnfα secretion by BMDM, in both juxtacrine and paracrine culture (Fig. 3D, 3E). These differential secretion profiles were observed only with cytokine activation in coculture, with undetectable cytokine levels detected in the unstimulated condition and with 3T3 alone. In summary, 3T3 coculture promotes BMDM secretion of IL-10 in a contact-dependent manner, and suppresses Tnfα via paracrine signaling.

Macrophages enhance 3D puncture wound closure by 3T3 fibroblasts in collagen gels. In the body, cells interact within the 3D environment of extracellular matrix (ECM). To examine macrophage-fibroblast interaction in a more physiologic system, we embedded 3T3 and/or BMDM in soft collagen hydrogels and examined reciprocal cellular effects. After 3 days of 'healing' we observed a greater reduction in puncture wound area with 3T3-BMDM coculture, compared to 3T3 alone, further supporting the hypothesis that BMDM facilitate fibroblast response to injury (Fig. 4A, 4B). Similar to 2D coculture, 3T3 in wounded hydrogels modulated BMDM to a pro-healing phenotype, with greater secreted IL-10 and reduced Tnfα, compared to BMDM alone (Fig. 4C).

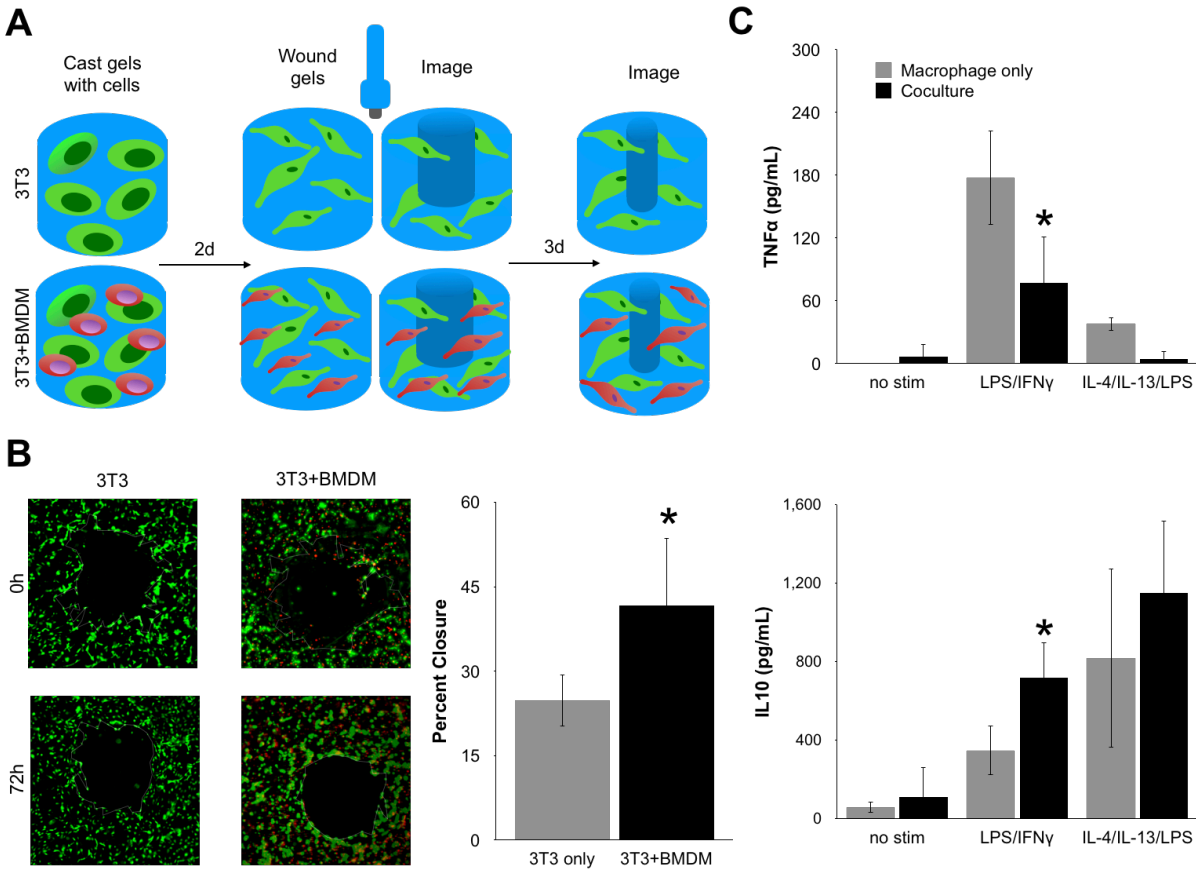

Figure 4. BMDM enhance 3T3 wound closure in 3D. A) Schematic of 3D collagen gel culture of 3T3 and BMDM, and puncture wounding. B) Maximum intensity projection micrographs and quantification showing wound closure of 3T3 in collagen gels with or without BMDM, visualized using cell tracker green. C) Tnfα and IL-10 cytokine secretion from BMDM in collagen gels with or without 3T3. *indicates $p<0.05$ with student's t-test, compared to monoculture with same cytokine stimulation.

Discussion

In this study, we have shown that BMDM promote 3T3 fibroblast wound closure in 2D and 3D. Further, we observed evidence of contact dependence in coculture-enhanced 3T3 scratch wound closure and BMDM IL-10 secretion. Two potential mechanisms behind these effects were explored, gap-junction mediated intercellular signaling was explored, yielding evidence that gap junction signaling may play a role in coculture-enhanced BMDM IL-10 secretion. Together, these results support a role for reciprocal juxtacrine interactions between macrophages and fibroblasts, governing cell behaviors independent of paracrine factors.

The contact dependent behaviors observed in this study pose an interesting puzzle. The 3T3 fibroblast enhanced IL-10 secretion was physically driven, but not the suppressed Tnfα response. IL-10 is known to suppress LPS/TLR induced Tnfα secretion in macrophages via Stat3, a cytoplasmic signaling protein also regulated by cytokines IL-6, IL-27, in macrophages (Lang, 2005). This plurality may explain the suppression of Tnfα in paracrine coculture, despite the absence of enhanced IL-10 secretion. The observation of fibroblast induced anti-inflammatory polarization of BMDM is also supported by the analogous finding that human synovial fibroblasts suppress Tnfα induced inflammatory polarization of human macrophages, modulating about one third of TNF-regulated genes in the macrophage population, as assessed by global transcriptome analysis (Fig. 3 C,D) (Donlin et al., 2014). In a disease context, human dermal fibroblasts have also been shown to promote anti-inflammatory polarization of human macrophages and improve skin wound healing when injected intradermally in db/db diabetic mice (Ferrer et al., 2017). It has also been shown that macrophage secretion of IL-10 is, in part, regulated by mechanical stimulation in a variety of contexts, notably higher on soft substrates, compared to stiff substrates, providing further support for physical regulation shown in our study (McWhorter et al., 2015). Our observations of fibroblast modulation of macrophage cytokine secretion through juxtacrine vs. paracrine coculture add complexity to the existing picture painted in the literature.

In the other direction, macrophage enhancement of fibroblast wound closure was also contact dependent, and additionally affected by macrophage activation. We found that unstimulated macrophages were potent enhancers of 3T3 scratch closure at all coculture ratios, whereas activated macrophages showed a dose dependent response (Fig. 1, 2). The reason for this discrepancy is unclear, but it confounded the investigation of contact dependence in activated macrophage-enhanced fibroblast scratch wound closure; the paracrine transwell coculture system was constrained to a 1:5 ratio, which was insufficient to induce an effect on scratch closure with the addition of stimulating cytokines. Macrophage-fibroblast ratio has also been shown to influence contractile fibroblast phenotype induction and macrophage polarization in a spheroid coculture system (Tan et al., 2020). Thus, if macrophage polarization suppressed physical cell-cell signaling, a higher threshold ratio of macrophages would be needed to promote fibroblast scratch wound closure. These data point to a complex interplay of physical and biochemical interactions between macrophages and fibroblasts, affecting behaviors in both cell types.

In summary, 2D and 3D in vitro wound assays were used to characterize a novel contact dependent macrophage enhancement of 3T3 wound closure and reciprocal augmentation of IL-10 secretion. Mechanisms of macrophage-fibroblast physical signaling remain poorly understood, although these cell types may establish contact in several ways, including via gap junctions and adhesion via integrin/CAMs, which may be transduced though mechanosensitive ion channels (Dean et al., 1988). Additionally, paracrine-mediated suppression of Tnfα secretion was also observed in this study, highlighting potential redundancies in intercellular signaling. Ultimately, a combination of in vitro and in vivo tools are needed to appreciate both phenotypic effects and mechanistic complexity of macrophage-fibroblast communication, and for application to clinical needs. Better understanding these interactions between key wound effector cell types may provide targets for rational development of novel wound therapies.

Future directions

Perform scRNAseq on cocultured cells and compare transcriptional profile to monoculture controls to screen for mechanotransduction pathways activated by coculture. Alternatively, separate cocultured cells by FACS or magnetic bead separation and perform bulk RNAseq.

Examine the role of matrix composition and stiffness on 3D wound closure and macrophage polarization in coculture.

Automate wound closure quantification in 2D and 3D

Probe effects of stimulation on wound closure in 3D

Use cytoskeletal inhibitors to determine the role of cellular traction forces on contact-dependent coculture effects

References

Boddupalli, A., Zhu, L., and Bratlie, K.M. (2016). Methods for Implant Acceptance and Wound Healing: Material Selection and Implant Location Modulate Macrophage and Fibroblast Phenotypes. Adv Healthc Mater *5*, 2575-2594.

Boniakowski, A.E., Kimball, A.S., Jacobs, B.N., Kunkel, S.L., and Gallagher, K.A. (2017). Macrophage-Mediated Inflammation in Normal and Diabetic Wound Healing. J Immunol *199*, 17-24.

Brazil, J.C., Quiros, M., Nusrat, A., and Parkos, C.A. (2019). Innate immune cell-epithelial crosstalk during wound repair. J Clin Invest *129*, 2983-2993.

Dean, M.F., Cooper, J.A., and Stahl, P. (1988). Cell Contact and Direct Transfer between Co-Cultured Macrophages and Fibroblasts. J Leukoc Biol *43*, 539-546.

Donlin, L.T., Jayatilleke, A., Giannopoulou, E.G., Kalliolias, G.D., and Ivashkiv, L.B. (2014). Modulation of TNF-induced macrophage polarization by synovial fibroblasts. J Immunol *193*, 2373-2383.

Eming, S.A., Martin, P., and Tomic-Canic, M. (2014). Wound repair and regeneration: mechanisms, signaling, and translation. Sci Transl Med *6*, 265sr266.

Ferrer, R.A., Saalbach, A., Grünwedel, M., Lohmann, N., Forstreuter, I., Saupe, S., Wandel, E., Simon, J.C., and Franz, S. (2017). Dermal Fibroblasts Promote Alternative Macrophage Activation Improving Impaired Wound Healing. Journal of Investigative Dermatology *137*, 941-950.

Glaros, T., Larsen, M., and Li, L. (2009). Macrophages and fibroblasts during inflammation, tissue damage and organ injury. Front Biosci (Landmark Ed) *14*, 3988-3993.

Holt, D.J., Chamberlain, L.M., and Grainger, D.W. (2010). Cell–cell signaling in co-cultures of macrophages and fibroblasts. Biomaterials *31*, 9382-9394.

Kassebaum, N.J., Smith, A.G.C., Bernabe, E., Fleming, T.D., Reynolds, A.E., Vos, T., Murray, C.J.L., Marcenes, W., and Collaborators, G.B.D.O.H. (2017). Global, Regional, and National Prevalence, Incidence, and Disability-Adjusted Life Years for Oral Conditions for 195 Countries, 1990-2015: A Systematic Analysis for the Global Burden of Diseases, Injuries, and Risk Factors. J Dent Res *96*, 380-387.

Kloc, M., Ghobrial, R.M., Wosik, J., Lewicka, A., Lewicki, S., and Kubiak, J.Z. (2019). Macrophage functions in wound healing. J Tissue Eng Regen Med *13*, 99-109.

Lang, R. (2005). Tuning of macrophage responses by Stat3-inducing cytokines: molecular mechanisms and consequences in infection. Immunobiology *210*, 63-76.

Martinengo, L., Olsson, M., Bajpai, R., Soljak, M., Upton, Z., Schmidtchen, A., Car, J., and Jarbrink, K. (2019). Prevalence of chronic wounds in the general population: systematic review and meta-analysis of observational studies. Ann Epidemiol *29*, 8-15.

McWhorter, F.Y., Davis, C.T., and Liu, W.F. (2015). Physical and mechanical regulation of macrophage phenotype and function. Cell Mol Life Sci *72*, 1303-1316.

O'Rourke, S.A., Dunne, A., and Monaghan, M.G. (2019). The Role of Macrophages in the Infarcted Myocardium: Orchestrators of ECM Remodeling. Front Cardiovasc Med *6*, 101.

Sakar, M.S., Eyckmans, J., Pieters, R., Eberli, D., Nelson, B.J., and Chen, C.S. (2016). Cellular forces and matrix assembly coordinate fibrous tissue repair. Nat Commun *7*, 11036.

Sen, C.K., Gordillo, G.M., Roy, S., Kirsner, R., Lambert, L., Hunt, T.K., Gottrup, F., Gurtner, G.C., and Longaker, M.T. (2009). Human skin wounds: a major and snowballing threat to public health and the economy. Wound Repair Regen *17*, 763-771.

Tan, Y., Suarez, A., Garza, M., Khan, A.A., Elisseeff, J., and Coon, D. (2020). Human fibroblast-macrophage tissue spheroids demonstrate ratio-dependent fibrotic activity for in vitro fibrogenesis model development. Biomater Sci *8*, 1951-1960.

Witherel, C.E., Abebayehu, D., Barker, T.H., and Spiller, K.L. (2019). Macrophage and Fibroblast Interactions in Biomaterial-Mediated Fibrosis. Adv Healthc Mater *8*, e1801451.

Wong, V.W., Gurtner, G.C., and Longaker, M.T. (2013). Wound healing: a paradigm for regeneration. Mayo Clin Proc *88*, 1022-1031.

Chapter 3. Contact-dependent mechanisms of macrophage-fibroblast signaling in coculture

Introduction

Wound healing involves communication between various wound effectors, notably macrophages and fibroblasts. Both cell types are essential for normal progression of healing, and each serves unique functions in this process (Ferrer et al., 2017). As described in the previous chapter, the interaction between these macrophages and fibroblasts promotes wound healing, and involves both biophysical and biochemical cues. Fibroblast-mediated suppression of macrophage inflammatory activation has been described empirically in many tissues, primarily by measuring decreased secretion of TNFa and related cytokines, and increased secretion of IL-10, and similar pro-healing markers (Donlin et al., 2014; Holt et al., 2010). Conversely, macrophages have been shown to promote fibroblast chemotaxis and alignment, and modulate their fibrotic potential in a ratio-dependent manner (Bromberek et al., 2002; Tan et al., 2020). However, the mechanisms behind these reciprocal interactions remain unclear, and difficult to probe experimentally. Coculture of bone marrow derived macrophages (BMDM) and NIH 3T3 fibroblasts in a 2D monolayer in vitro provides a useful platform to parse these interactions with high throughput, additionally minimizing confounding variables such as influence of other cell types.

The myriad potential mechanisms behind the observed effects of coculture on macrophages and fibroblasts can be daunting to approach at first. While many paracrine and autocrine signaling pathways have been tied to the wound healing process, the role of contact-dependent intercellular signaling remains especially obscure, and thus presents a compelling target to explore. Gap junctions are a common means of intercellular communication via exchange of ions and small molecules, and are known to play a role in wound healing (Lembong et al., 2017; Willebrords et al., 2016; Wong et al., 2016). Macrophages and fibroblasts both express connexin 43, as well as cell type-specific connexins, the building blocks of gap junctions,

and heterohexameric structures are known to form commonly (Cottrell and Burt, 2005; Dean et al., 1988; Oviedo-Orta and Howard Evans, 2004). Additionally, ion flux, primarily calcium, is known to play a role in macrophage activation, and fibroblast mechanosensing (Godbout et al., 2013; Santoni et al., 2018). Therefore, gap junctions appear to be one mechanism to consider for propagation of contact-dependent signaling between macrophages and fibroblasts.

In addition to direct communication through gap junctions, there are ample data to suggest that macrophages and fibroblasts may employ mechanosensing of cell-cell contact to generate reciprocal signaling. In macrophages, activation of calcium permeant mechanosensitive ion channels PIEZO1, TRPV4 and TRPV7 has been shown to facilitate calcium influx required for LPS-induced and TLR4-mediated macrophage inflammatory activation (Dutta et al., 2020; Schappe et al., 2018). PIEZO1 in particular, is more highly expressed in macrophages compared to other mechanosensitive ion channels, and was recently shown to be critical for macrophage activation and inflammation in the lung following injury or infection (Solis et al., 2019). Adjacently, calcium oscillations in fibroblasts propagate through 2D monolayers, and respond to both wounding and substrate stiffness, mediated by cellular traction force (Lembong et al., 2017). With strong evidence for mechanically driven calcium signaling in both macrophage activation and fibroblast wound response, the effect of coculture of these two cell types on their calcium signaling is the next frontier of investigation.

In this study, gap junctions and calcium flux were found to contribute to macrophage fibroblast interactions in the context of 2D scratch wound closure. Inhibition of gap junctions with small molecule palmitoleic acid attenuated the coculture-enhanced BMDM secretion of IL-10 upon activation with IL-4, IL-10, and LPS compared to monoculture. However, neither palmitoleic acid nor peptide gap junction inhibitor GAP26 affected BMDM-enhanced 3T3 scratch wound closure, in contrast to complete abrogation with knockout of mechanosensitive ion channel PIEZO1 in BMDM. Finally, fibroblast coculture enhanced BMDM calcium flux, an effect attenuated by the

addition of palmitoleic acid. These results highlight a combination of biophysical, ionic, and biochemical mechanisms which may govern macrophage-fibroblast interactions, in the context of 2D scratch wound healing.

Methods

Cell Culture: NIH 3T3 fibroblasts were cultured below 85% confluence in DMEM complete media (DMEM+glucose+pyruvate+Gln (Corning), 10% HI-FBS (Gibco), 1% Penicillin streptomycin, L-Glutamine (Gibco)) and used at passage 3-12. For 2D coculture experiments, 3T3 were stained with DiO or DiI membrane stain (Fisher, 5uL/mL) for 40 min in DMEM basal media at 37 C and washed twice with DMEM complete before use.

Bone marrow derived macrophages were derived from mouse bone marrow monocytes, differentiated for 7 days in D10 media (DMEM, 10% HI-FBS, 1% Penicillin streptomycin, L-Glutamine (Gibco), 10% M-CSF L929 conditioned media). Fluorescently labelled BMDM were derived from LysMCre$^{+/-}$; TdTomato$^{fl/+}$ mice, courtesy the Plikus lab. BMDM were isolated from LysMCre$^{+/-}$; Piezo1$^{fl/fl}$ mice and LysMCre$^{+/-}$; Piezo1$^{fl/+}$mice to for Piezo1 knock out studies. For calcuium imaging, BMDM were isolated from LysMCre$^{+/-}$; SALSA6f$^{fl/fl}$ mice expressing calcium reporter transgene SALSA6f. Collection of primary cells for culture adhered to institutional IACUC protocol AUP 20-047.

Genotype	Use
LysMCre$^{+/-}$; tdTomato$^{fl/+}$	tdTomato Labeled BMDM for coculture
LysMCre$^{+/-}$; Piezo1$^{fl/fl}$	Piezo1 knock out BMDM and heterozygote for coculture
LysMCre$^{+/-}$; SALSA6f$^{fl/fl}$	Ratiometric calcium reporter in BMDM

Table 2. Catalogue of transgenic mice

2D Scratch assay and coculture: Membrane labelled 3T3 fibroblasts in DMEM complete media were seeded at 7.9e4 cells/cm^2 in a fibronectin (10ug/mL) coated 24-well polystyrene well plate and allowed to adhere for 3 hours. For coculture conditions, BMDM were suspended in DMEM complete and seeded on top of the 3T3 monolayer. After allowing adhesion for an additional 4 hours, cultures were stimulated with activating cytokines overnight (LPS/IFNg

10ng/mL, or IL-4/IL-13 20ng/mL +LPS 10ng/mL (Fisher, R&D systems, Biolegend)). Subsequently, vertical scratches were made, one per well, using a 10ul pipette tip, and cultures were imaged at 0h and 6h following scratch, using the 4x objective on an Olympus inverted fluorescence microscope. Area of scratch in paired single frames was measured at 0h and 6h, in triplicate per condition, and the difference in area between time points was designated area closed.

Cytokine Quantification: Biolegend ELISA kits for mouse IL-10 and TNFa were used to determine concentrations of these cytokines in the supernatant, collected 6h after scratch, and were used as directed by the manufacturer.

Functional studies: For gap junction studies, inhibitors palmitoleic acid ([50 or 100uM], Fisher) or GAP26 (50uM, Tocris) were added to culture overnight prior to scratch assay. For prostaglandin studies, PGE2 or EP2 receptor inhibitor PF044 (50-100uM, Sigma) were added overnight prior to scratch assay. Wnt5a (5ug/mL) was added immediately prior to scratching.

Calcium imaging and analysis: BMDM isolated from LysMCre$^{+/-}$; SALSA6f$^{fl/fl}$ mice were cultured at 5e4/cm^2 in fibronectin coated 35mm dishes with 14mm glass bottom inset. Phenol free DMEM complete was used. For coculture studies, equal number of 3T3 fibroblasts were seeded simultaneously. Cells were allowed to adhere for 6 hours, then stimulated with palmitoleic acid (100uM) if applicable, and incubated overnight prior to imaging. Confocal imaging of calcium dynamics in Salsa6f BMDM was conducted using an Olympus Fluoview FV3000RS confocal laser scanning microscope equipped with a high-speed resonance scanner and IX3-ZDC2 Z-drift compensator (Stem Cell Research Core, UCI SOM). Laser excitation at 488nm and 561nm was used to image cultures through an Olympus 40xsilicone oil objective (NA 1.25) at 1fps for 10 min per field of view. Ratiometric quantification of calcium flux was performed via ImageJ software (Rueden et al., 2017; Schindelin et al., 2012), normalizing green calcium signal to red cytoplasmic

signal and thereby reducing the impact of green signal changes unrelated to calcium flux. In brief, ImageJ was used to trace and quantify subcellular regions showing calcium flux, to determine number of events/(cell*min) and percent of cells in the FOV with active calcium flux using a threshold of 2.5 times higher than baseline.

Results

To assess the role of gap junctions in cell-cell interactions, fibroblasts and murine BMDMs were sequentially seeded and stimulated with activating cytokines, then scratched and imaged after overnight treatment with gap junction inhibitors palmitoleic acid or GAP26. The effect of coculture on macrophage calcium flux was visualized by seeding SALSA6f expressing BMDM with or without 3T3 in glass bottom dishes in phenol free DMEM complete, and live imaging with confocal microscopy. The role of gap junctions in calcium flux was interrogated by adding palmitoleic acid overnight prior to calcium imaging.

Role of GAP junctions in macrophage-fibroblast interactions. We set out to find a contact-dependent mechanism by which macrophages and fibroblasts interact, one that could be responsible for the coculture-enhanced 3T3 wound closure and pro-healing polarization of BMDM described in Chapter 2. Gap junctions are a common means of intercellular communication between cells and are known to be involved in wound healing (Becker et al., 2012). As macrophages and fibroblasts both express connexins, the building blocks of gap junctions, and calcium influx has been shown to occur with macrophage activation, gap junctions appeared a suitable target for investigation (Dean et al., 1988; Hulsmans et al., 2017; Oviedo-Orta and Howard Evans, 2004). The inhibition of gap junctions, using small molecule palmitoleic acid or peptide GAP26, did not affect scratch closure of 3T3 in monoculture or coculture with BMDM (Fig. 1A, 1B). In contrast, the observed increase in IL-10 secretion in coculture, but not decrease in TNFa, was abrogated by palmitoleic acid (Fig. 1C, 1D). This finding aligned with our earlier observation that suppression of TNFa can be achieved with both 2D paracrine and juxtacrine coculture, whereas the increase in IL-10 secretion was dependent on BMDM-3T3 contact found only in juxtacrine coculture (Ch. 2 Fig. 2C, 2D). These data suggest that gap junctions may have a role in IL-10 modulation in BMDM-3T3 coculture.

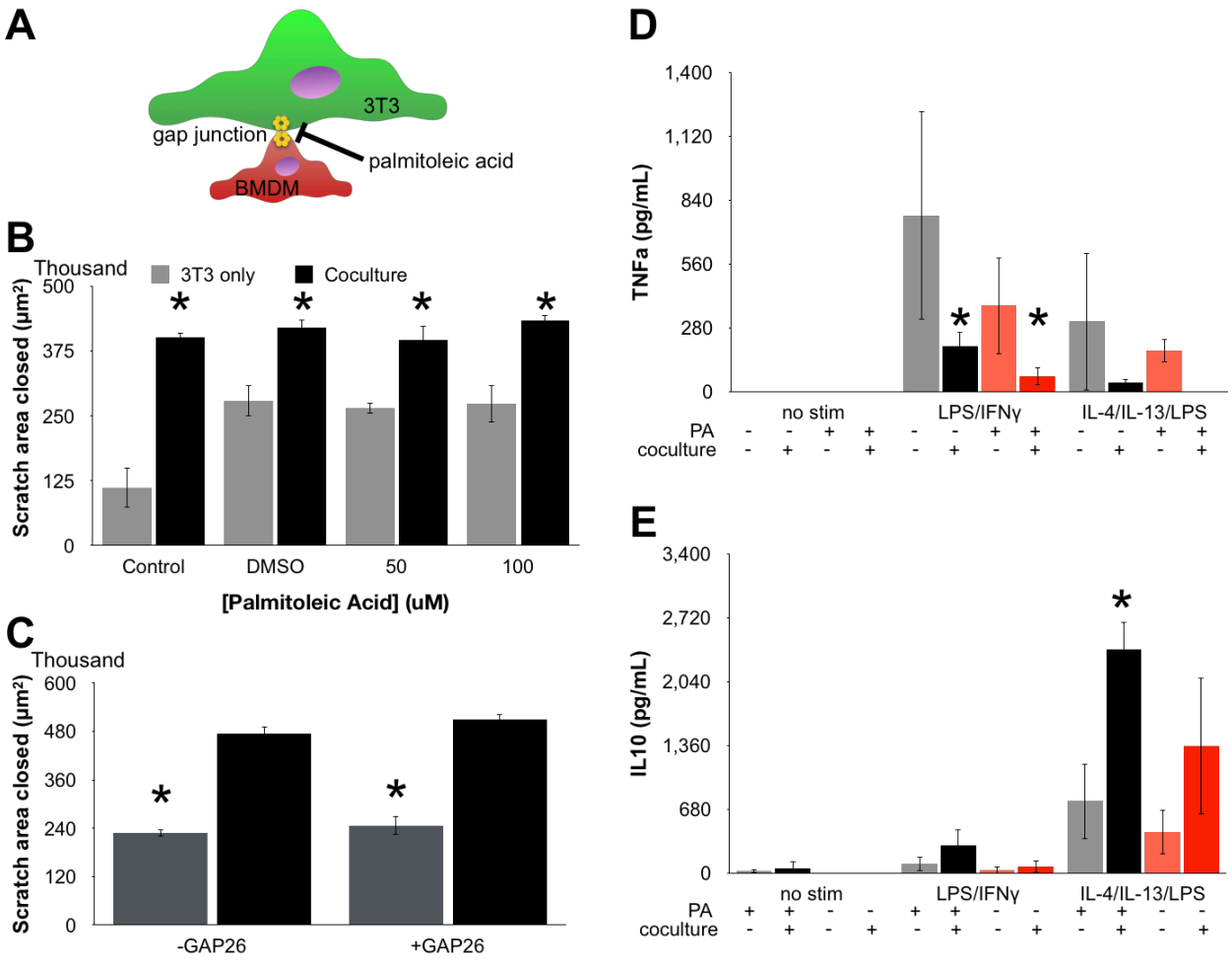

Figure 10. Inhibition of gap junctions attenuates coculture enhanced IL-10 secretion, but not scratch closure. A) Schematic of gap junction between macrophage and 3T3 fibroblast. (B,C) Scratch closure in mono and coculture with B)palmitoleic acid or C) GAP26, a peptide gap junction inhibitor. D)TNFa and E) IL-10 BMDM cytokine secretion in the presence or absence of 3T3 coculture and 50uM palmitoleic acid. *indicates $p<0.05$ with student's t-test, compared to monoculture with same stimulation.

Mechanosensitive ion channel PIEZO1 may play a role in macrophage-fibroblast interactions. The contact-dependence of a subset of coculture-driven behaviors, described in Chapter 2, presents a potential role for mechanotransduction in this interaction, in addition to direct communication via gap junctions. PIEZO1 is the predominant mechanosensitive ion channel expressed in BMDM, making is a prime target for investigating this aspect of macrophage-fibroblast interactions (Solis et al., 2019). PIEZO1 knock out BMDM from Piezo1$^{fl/fl}$;

LysMCre$^{+/-}$ transgenic mice suppressed BMDM-enhanced 3T3 scratch closure, compared to wild type and heterozygote flox controls, indicating that (Fig. 2). While there are many components at play, this finding suggests that PIEZO1 has a role in producing contact-mediated effects of macrophage-fibroblast coculture.

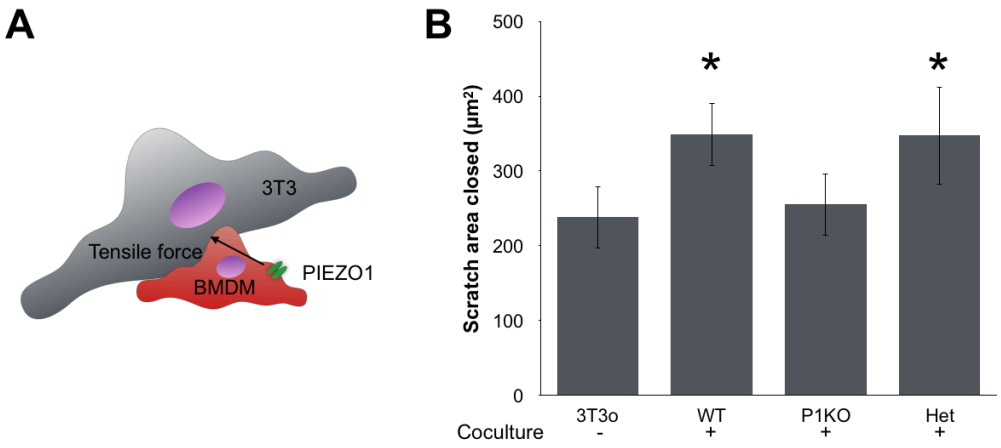

Figure 11. PIEZO1 knock out suppresses BMDM enhanced 3T3 scratch closure. A) Schematic showing BMDM PIEZO1 ion channel mechanically activated by cell-cell contact. B) Fibroblast scratch wound closure in monoculture and coculture with wild type (WT), SALSA6f$^{fl/fl}$ LysMCre$^{+/-}$(P1KO), or heterozygote control (Het) BMDM. *indicates $p<0.05$ with student's t-test, compared to monoculture.

BMDM calcium flux enhanced with fibroblast coculture. The functional role of gap junctions in macrophage-fibroblast interactions was more directly probed by visualizing calcium flux, using BMDM derived from SALSA6f$^{fl/fl}$ LysMCre$^{+/-}$ transgenic mice (Dong et al., 2017). The SALSA6f transgene encodes a ratiometric calcium reporter fusion protein containing cytoplasmic label tdTomato and calcium sensitive GCaMP6f. Calcium imaging of SALSA6f BMDMs with 3T3 coculture showed increased in calcium events/minute and proportion of active cells; overnight treatment with palmitoleic acid abrogated coculture enhancement (Fig. 3). Coculture additionally increased amplitude of calcium signals compared to baseline, and this observation was also attenuated by palmitoleic acid. These results provide evidence that calcium flux contributes to the contact-dependent interactions between macrophages and fibroblasts.

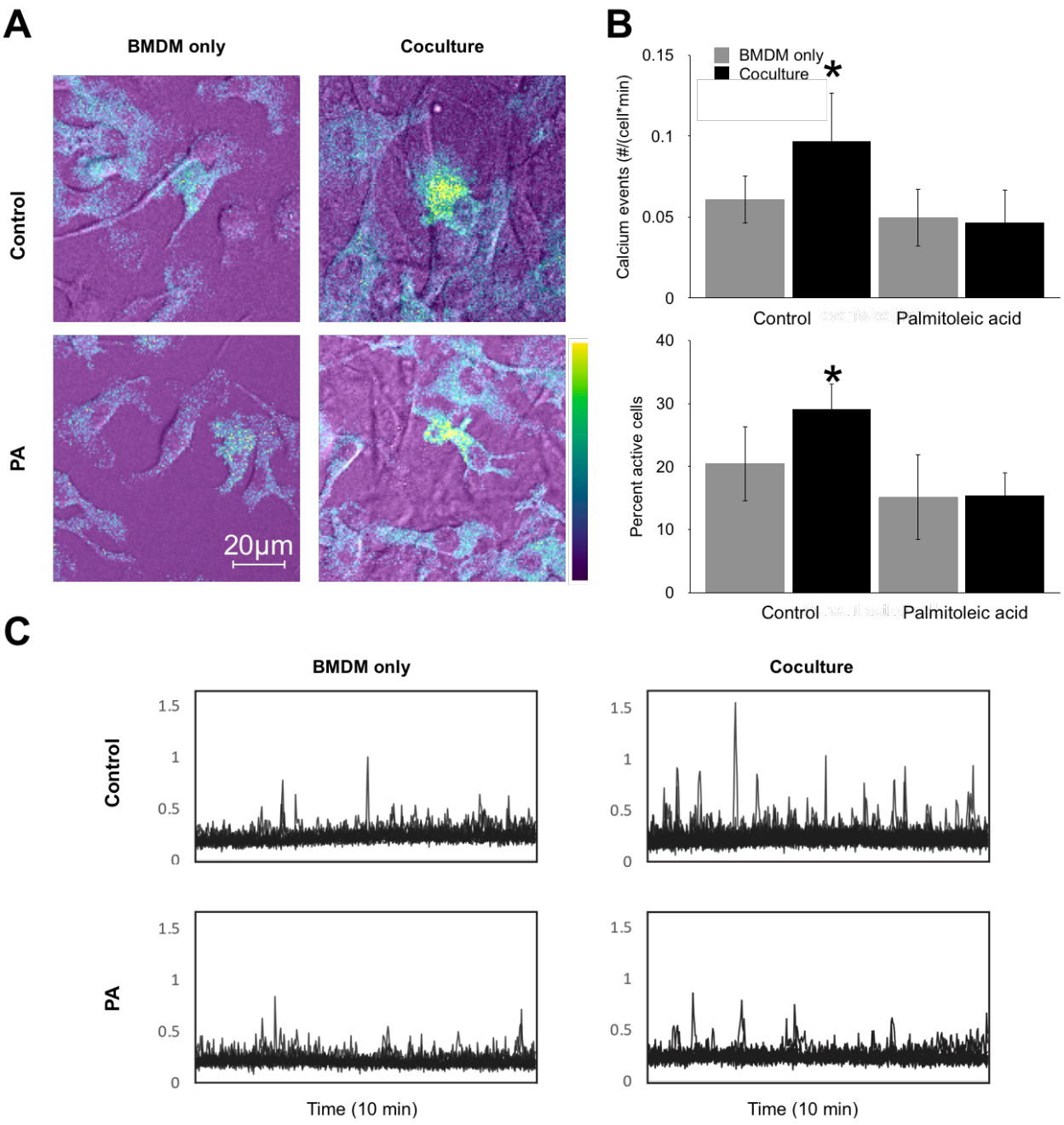

Figure 12. BMDM calcium signaling enhanced with 3T3 coculture, and abrogated with palmitoleic acid. A) Ratiometric calcium signals in SALSA6f expressing BMDM with or without 3T3 coculture, after overnight control and palmitoleic acid treatment. Yellow indicates high calcium, blue indicates low calcium. B) Frequency of BMDM calcium events per cell per minute and proportion of BMDM with active calcium signals greater than 2.5 fold above baseline, in the presence or absence of coculture or palmitoleic acid. C) Overlayed calcium signal traces of individual cells over time, in the presence or absence of coculture or palmitoleic acid. *indicates $p<0.05$ with student's t-test, compared to monoculture with same treatment.

Discussion

In this study, the inhibition of gap junctions via palmitoleic acid was found to abrogate 3T3 coculture-enhanced secretion of IL-10. Neither palmitoleic acid nor peptide gap junction inhibitor GAP26 attenuated coculture enhanced fibroblast scratch closure; however, PIEZO1 knock out BMDM failed to promote fibroblast scratch closure in coculture, compared to heterozygote and wild type BMDM controls. Live calcium imaging showed an enhanced number of calcium events and higher proportion of active BMDM in coculture, compared to monoculture, an enhancement diminished by the addition of palmitoleic acid. These findings support a role for both gap junctions and calcium-dependent signaling in reciprocal coculture effects in macrophages and fibroblasts.

Despite promising empirical findings, mechanisms of macrophage-fibroblast physical signaling to macrophages are poorly described in the literature (Dean et al., 1988). Macrophages and fibroblasts may establish contact in several ways, including via gap junctions and adhesion via integrin/CAMs, which may be transduced though mechanosensitive ion channels. Previous studies have shown that both cell types express connexin 43 and form gap junctions in monoculture, and heterohexameric gap junctions also form commonly (Cottrell and Burt, 2005; Oviedo-Orta and Howard Evans, 2004). Our finding that palmitoleic acid inhibition of gap junctions abrogates coculture-enhanced IL-10 secretion supports this mechanism as a contributor to contact-dependent macrophage-fibroblast signaling (Fig. 1). However, the lack of effect on fibroblast scratch closure by both palmitoleic acid and GAP26 implies that a gap junction independent mechanism mediates this behavior. In fact, mechanosensitive ion channel PIEZO1 may fill the role, as BMDM from $Piezo1^{fl/fl}$; $LysmCre^{+/-}$ mice did not produce enhanced 3T3 scratch closure, in contrast to wild type and heterozygote BMDM controls (Fig. 2). These results highlight the multi-faceted nature of macrophage-fibroblast interactions.

To pursue a final common pathway for coculture-induced behaviors, live-cell confocal microscopy was used to visualize calcium flux in SALSA6f expressing BMDM with and without 3T3 coculture. Increase in frequency of events, proportion of active BMDM, and amplitude of calcium signals with coculture supports a role for calcium in macrophage-fibroblast signaling. The role of ion transfer in response to physical cues is further supported by the observed PIEZO1 dependence of coculture-enhanced scratch closure, and previously published finding that calcium oscillation frequency is proportional to mechanical challenge in myofibroblasts (Godbout et al., 2013).

On the other hand, the observation of suppressed TNFa secretion with macrophage-fibroblast coculture stands in contrast to studies associating calcium influx in with macrophage inflammatory activation. BMDM from TRPM7-inactivated mice were shown to produce increased IL-10 and TNFa, and induce pro-fibrotic phenotype in WT cardiac fibroblasts (Rios et al., 2020). However, neither macrophage nor fibroblast calcium flux assessed in this study, leaving open the possibility that effects of TRPM7 inactivation were calcium-independent. Additionally, coculture suppressed TNFa secretion was observed independent of cell-cell contact, suggesting that this behavior may be paracrine and not calcium-channel mediated (Ch. 2 Fig. 2)(Schappe et al., 2018). These and other studies of paracrine signaling between macrophages and fibroblasts indicate a multifactorial interaction with the potential for combinatorial effects (Holt et al., 2010).

Our findings suggest that gap junctions and PIEZO1 are two structures mediating direct macrophage-fibroblast communication, potentially mediating contact-dependent increase in macrophage calcium signaling, enhanced 3T3 scratch wound closure and fibroblast coculture augmented IL-10 secretion.

Future directions

Measure the effect of coculture on SALSA6f fibroblast calcium flux

Measure the effect of cytokine stimulation on coculture enhanced calcium events

Examine magnitude and localization of events

Optimize calcium imaging of wounded cocultures

Consider probing role of particular structures – gap junction reporter, P1KO SALSA, etc.

References

Becker, D.L., Thrasivoulou, C., and Phillips, A.R. (2012). Connexins in wound healing; perspectives in diabetic patients. Biochim Biophys Acta *1818*, 2068-2075.

Bromberek, B.A., Enever, P.A., Shreiber, D.I., Caldwell, M.D., and Tranquillo, R.T. (2002). Macrophages influence a competition of contact guidance and chemotaxis for fibroblast alignment in a fibrin gel coculture assay. Exp Cell Res *275*, 230-242.

Cottrell, G.T., and Burt, J.M. (2005). Functional consequences of heterogeneous gap junction channel formation and its influence in health and disease. Biochim Biophys Acta *1711*, 126-141.

Dean, M.F., Cooper, J.A., and Stahl, P. (1988). Cell Contact and Direct Transfer between Co-Cultured Macrophages and Fibroblasts. J Leukoc Biol *43*, 539-546.

Dong, T.X., Othy, S., Jairaman, A., Skupsky, J., Zavala, A., Parker, I., Dynes, J.L., and Cahalan, M.D. (2017). T-cell calcium dynamics visualized in a ratiometric tdTomato-GCaMP6f transgenic reporter mouse. Elife *6*.

Donlin, L.T., Jayatilleke, A., Giannopoulou, E.G., Kalliolias, G.D., and Ivashkiv, L.B. (2014). Modulation of TNF-induced macrophage polarization by synovial fibroblasts. J Immunol *193*, 2373-2383.

Dutta, B., Arya, R.K., Goswami, R., Alharbi, M.O., Sharma, S., and Rahaman, S.O. (2020). Role of macrophage TRPV4 in inflammation. Lab Invest *100*, 178-185.

Ferrer, R.A., Saalbach, A., Grünwedel, M., Lohmann, N., Forstreuter, I., Saupe, S., Wandel, E., Simon, J.C., and Franz, S. (2017). Dermal Fibroblasts Promote Alternative Macrophage Activation Improving Impaired Wound Healing. Journal of Investigative Dermatology *137*, 941-950.

Godbout, C., Follonier Castella, L., Smith, E.A., Talele, N., Chow, M.L., Garonna, A., and Hinz, B. (2013). The mechanical environment modulates intracellular calcium oscillation activities of myofibroblasts. PLOS ONE *8*, e64560.

Holt, D.J., Chamberlain, L.M., and Grainger, D.W. (2010). Cell–cell signaling in co-cultures of macrophages and fibroblasts. Biomaterials *31*, 9382-9394.

Hulsmans, M., Clauss, S., Xiao, L., Aguirre, A.D., King, K.R., Hanley, A., Hucker, W.J., Wulfers, E.M., Seemann, G., Courties, G.*, et al.* (2017). Macrophages Facilitate Electrical Conduction in the Heart. Cell *169*, 510-522 e520.

Lembong, J., Sabass, B., and Stone, H.A. (2017). Calcium oscillations in wounded fibroblast monolayers are spatially regulated through substrate mechanics. Phys Biol *14*, 045006.

Oviedo-Orta, E., and Howard Evans, W. (2004). Gap junctions and connexin-mediated communication in the immune system. Biochim Biophys Acta *1662*, 102-112.

Rios, F.J., Zou, Z.G., Harvey, A.P., Harvey, K.Y., Nosalski, R., Anyfanti, P., Camargo, L.L., Lacchini, S., Ryazanov, A.G., Ryazanova, L.*, et al.* (2020). Chanzyme TRPM7 protects against cardiovascular inflammation and fibrosis. Cardiovasc Res *116*, 721-735.

Rueden, C.T., Schindelin, J., Hiner, M.C., DeZonia, B.E., Walter, A.E., Arena, E.T., and Eliceiri, K.W. (2017). ImageJ2: ImageJ for the next generation of scientific image data. BMC Bioinformatics *18*, 529.

Santoni, G., Morelli, M.B., Amantini, C., Santoni, M., Nabissi, M., Marinelli, O., and Santoni, A. (2018). "Immuno-Transient Receptor Potential Ion Channels": The Role in Monocyte- and Macrophage-Mediated Inflammatory Responses. Front Immunol *9*, 1273.

Schappe, M.S., Szteyn, K., Stremska, M.E., Mendu, S.K., Downs, T.K., Seegren, P.V., Mahoney, M.A., Dixit, S., Krupa, J.K., Stipes, E.J.*, et al.* (2018). Chanzyme TRPM7 Mediates the Ca(2+) Influx Essential for Lipopolysaccharide-Induced Toll-Like Receptor 4 Endocytosis and Macrophage Activation. Immunity *48*, 59-74 e55.

Schindelin, J., Arganda-Carreras, I., Frise, E., Kaynig, V., Longair, M., Pietzsch, T., Preibisch, S., Rueden, C., Saalfeld, S., Schmid, B.*, et al.* (2012). Fiji: an open-source platform for biological-image analysis. Nat Methods *9*, 676-682.

Solis, A.G., Bielecki, P., Steach, H.R., Sharma, L., Harman, C.C.D., Yun, S., de Zoete, M.R., Warnock, J.N., To, S.D.F., York, A.G.*, et al.* (2019). Mechanosensation of cyclical force by PIEZO1 is essential for innate immunity. Nature *573*, 69-74.

Tan, Y., Suarez, A., Garza, M., Khan, A.A., Elisseeff, J., and Coon, D. (2020). Human fibroblast-macrophage tissue spheroids demonstrate ratio-dependent fibrotic activity for in vitro fibrogenesis model development. Biomater Sci *8*, 1951-1960.

Willebrords, J., Yanguas, S.C., Maes, M., Decrock, E., Wang, N., Leybaert, L., Kwak, B.R., Green, C.R., Cogliati, B., and Vinken, M. (2016). Connexins and their channels in inflammation. Crit Rev Biochem Mol *51*, 413-439.

Wong, P., Tan, T., Chan, C., Laxton, V., Chan, Y.W., Liu, T., Wong, W.T., and Tse, G. (2016). The Role of Connexins in Wound Healing and Repair: Novel Therapeutic Approaches. Front Physiol *7*, 596.

Appendix A: Protocols

Cell culture of NIH/3T3 (ATCC CRL-1658)

Materials

- DMEM complete media (D3) (10% FBS, +100 ug/mL Penicillin/Streptomycin/Glutamine)
- DMEM only (no additives, no serum)
- 0.25% Trypsin-EDTA
- Sterile PBS
-Ionomycin
-DiO membrane stain

Passaging from T75 flask

1. Wash monolayer with Sterile PBS
2. Add 1-3ml 0.25% trypsin-EDTA
3. Incubate at 37C for 3-5 min
4. Use additional 5 mL DMEMcomplete to blow cells off of attached surface.
5. Transfer cells to 15 mL conical and spin 1000xg for 5 min to pellet
6. Aspirate supernatant and resuspend pellet in 5 mL DMEMcomplete, using 1 mL pipette to ensure uniform suspension
7. Count cells
   Seed at:
   1:5 (reaches confluence in 3-4 days)
   1:3 (reaches confluence in 2 days)

Staining 3T3 with DiO from T75 flask

1. Wash monolayer with PBS
2. Add 1-3ml 0.25% trypsin-EDTA
3. Incubate at 37C for 3-5 min
4. Use additional 5 mL DMEMcomplete to blow cells off of attached surface.
5. Transfer cells to 15 mL conical and spin 1000xg for 5 min to pellet
6. Resuspend pellet in 3 mL DMEMonly (serum free) [~1e6 cells/mL]
7. Add 15uL DiO (5uL dye/mL cells)
8. Allow to stain at 37C for 30 min
9. Add 5 mL DMEMcomplete to quench, and spin 1000xg for 5 min to pellet.
10. Resuspend in 5 mL DMEMcomplete
11. Count

Ionomycin Apoptosis induction

1. Thaw ionomycin to liquid state.
2. Add 2uL/well in 6-well plate with 2mL media per well (1:1000 dilution)
3. Incubate 16H to and then use cell dissociation buffer to harvest for assays.

Seed at:

Scratch: 1.5e5/well in fibronectin coated 24-well plate

3T3m induction: 3e4/well in 12-well plate with glass coverslips

Apoptosis: 1.5e5/well in 6-well

Material preparation

Collagen:

		vol NaOH = vol collagen*0.023			
cells				0.1mg/mL	
vol (mL)	final conc (mg/mL)	NaOH (ul)	DMEMo+ Cells (ul)	fibronectin (ul)	collagen (ul)
1.5	6	54	-1067	150	2362
1.5	2	18	545	150	787
8	2	97	2904	800	4199
	all on ice, add:	1	collagen		
	mix well after each	2	DMEMo + cells		
		3	fibronectin		
		4	NaOH		volume (ul)
	mix well on ice, and add to multiwell plate to coat			6-well	960
	gel for 30 min at 37 deg C			12-well	480
	hydrate with complete media			24-well	240

GelMA:

			Final%		
GelMA	111	mg	20		
PBS (≥60C)	555	ul			
Irgacure 2959	16	mg	10		
methanol	160	ul			
combine 20% gelMA solution with 1% volume of 10%irgacure when ready to use					
volume 10% irgacure	5.55	ul			
keep warm while casting					
Photo crosslink with 365nm UV light for 1 min (3kPa) or 5min (150 kPa)					

PEGDA gel synthesis for implantation: May 2019

All solutions in PBS

Soft: 50% PEGDA-400

Stiff: 10% PEGDA-400

10% (0.05% Irgacure 2959)

1. Pipette 200uL of gel solution onto hydrophobic glass slide (Raji's bench). Lay 2 slides on top on either side of the droplet, and gently balance coverslip on top to form a disc of liquid between.
2. Crosslink with handheld UV or lightbox for 7 minutes. Soft gel will be cloudy.
3. Loosen gel with forceps and separate from glass.
4. Use 5mm punch to create discs and hydrate in PBS.
5. Divide in half to implant.

	PEGDA-400	PBS	0.05%Irgacure
Soft	100ul	800ul	100ul
Stiff	500ul	400ul	100ul

Cell isolation from wound tissue, for single cell RNA sequencing

	Wound tissue -> sequencing prep, pipeline						3.2.2020			Reagents to prep									
7:30															collagenase mix				
1h	punch wound, mince in 200uL PBS in petri dish						5x 3Tx			petri dishx3	PBS				9.7mL RPMI				
	add minced tissue to 10mL collagenase digest mix						3 tubes, one per Tx			three 15mL tubes with collagenase mix					0.027g Collagenase				
2h	shake at 37C for 2h, pipetting up and down every 15 min						rotator in Plikus lab			Tape					100uL 1M HEPES				
	Stop collagenase digest by adding 2mL 2%FBS									10 mL PBS+2%FBS					100uL 0.1M Sodium Pyruvate				
0.5h	Filter 70 and 40um filters									3x 15mL tubes									
1100	spin 300xg 5min									3x 40um cell strainer									
0.5h	resuspend in 100uL Dead cell removal microbeads, 15min RT						3 columns one per Tx			dead cell removal kit									
1h	prepare positive selection column									3x MS or LS column									
	add binding buffer to cell suspension, and add to column									binding buffer 60mL									
	rinse column with binding buffer																		
12:30	spin 300xg 5min, email HTGF 30min prep																		
	resuspend in 1mL cold 0.04% BSA						3 tubes, one per Tx			10mL 0.04% BSA									
0.5h	count, dilute to 1e6/mL									Hemacytometer, trypan blue, tubes									
										P1000, P200 pipettes and tips									
1300	deliver to HTGF						1300												

Protocol for frozen tissue section block preparation

Materials:

Tissue-Tek* O.C.T. Compound (SAKURA FINETEK USA INC # 4583; available through VWR)

Dry ice and container

Plastic Molds (Thermo 12-20, or anything similar)

Forceps

Permanent marker

Method:

Place dry ice in container on bench; position dry ice as level as possible in the container.

Fill a mold halfway with OCT.

Place mold on top of dry ice and wait for a layer of solid to form (white crystals will form on the surface closest to the dry ice).

Place tissue in mold.

Position tissue closer to one face of the mold with forceps and indicate with an arrow on the outside of mold (sectioning will begin from that face).

If needed, add additional OCT to ensure that the tissue is covered with OCT on all sides.

Leave on dry ice until the entire block is white/solid.

Place in -80C until ready to section.

Alternatives: Some tissues (e.g. muscle) are susceptible to distortion during freezing. One can submerge a mold with tissue and OCT into liquid nitrogen for rapid freeze to avoid distortion.

IHC of frozen sections

Fix	PFA	15		min	
Wash	PBS	8	continue to exchange rinse until smell is gone		
Perm	0.2% Triton in PBS	5			
	PBS Tween 0.1%	2	2	2	tap off between
Block	1% BSA in PBStween	120	+5-10% serum of secondary host		
Primary	in 1% BSA in PBStween	o/n 4 deg	70ul/sample in block		
Wash	PBS Tween 0.1%	10	10	10	
Secondary	in 1% BSA in PBStween	60	+ Hoechst	+5-10% serum of secondary host	
Wash	PBS Tween 0.1%	10	10	10	
	milliQ	2			
Mount		30ul/sample fluoromount			
via Kosuke Yamage, Plikus lab, 2019					
Rev.A; 2019	R. Nagalla				

IHC panels:		Secondaries all 1:1000		
	488	**594**	**647**	**DAPI**
MP phenotype	iNOS rab	F4/80 rat	Arg goat	X
	ab15323 1:100	BM-8 50-112-94 1:200	ab60176 1:50	
MP YAP	YAP rab	F480 rat		X
	cst 14074S 1:200	BM-8 50-112-94 1:200		
MyoF/F	SMA rab		PDGFRa goat	X
	ab -5694 1:200			
	Donkey anti-rabbit IgG alexa 488		Goat anti-rab	IgG 647
	A21206		A21244	
	Rabbit anti-goat IgG 488	Donkey anti rat 594	Donkey anti-goat IgG 647	
	A11078	thermo A21209	A21447	
		Goat anti rat 594		
		A1107		